Cell Systems

Article

NOT-gated chimeric antigen receptor circuits in T and NK cells

Graphical abstract

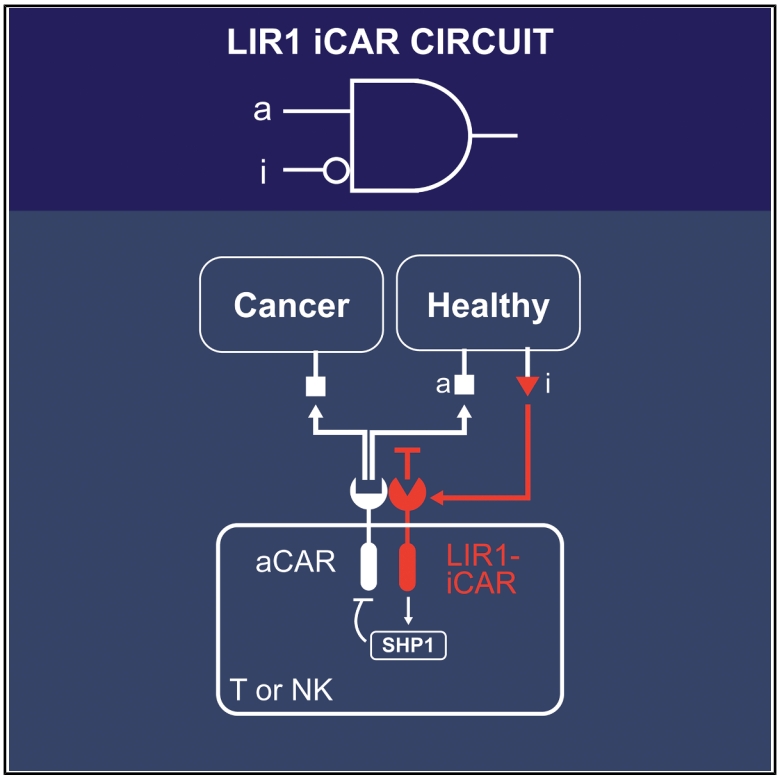

Authors

Seunghee Lee, Jingyao Chen, Menna Y. Siddiqui, ..., Tim K. Lu, Nicholas W. Frankel, Wilson W. Wong

Correspondence

nicholas.frankel@sentibio.com (N.W.F.), wilwong@bu.edu (W.W.W.)

In brief

Lee et al. present a screen of inhibitory CAR designs and identify LIR1 as the most promising intracellular signaling domain. The LIR1 iCAR functions in both T and NK cells, operates in *cis*, and transduces signaling via SHP1. iCAR can also reduce exhaustion phenotypes and potentially enhance antitumor responses.

Highlights

- Evaluate a large library of inhibitory CAR designs in T cells
- Demonstrate the LIR1 NOT-gate CAR designs in T and NK cells in mouse tumor models
- LIR iCAR operates in *cis*, and SHP1 is the key regulator of LIR iCAR signaling
- iCAR-expressing T cells display less exhaustion phenotype

Lee et al., 2026, Cell Systems *17*, 101561
April 15, 2026
https://doi.org/10.1016/j.cels.2026.101561

CellPress

Cell Systems

CellPress

Article

NOT-gated chimeric antigen receptor circuits in T and NK cells

Seunghee Lee,[1] Jingyao Chen,[1] Menna Y. Siddiqui,[1] Jaehoon Choi,[1] Joey Huang,[1] Derrick Lee,[2] Chen-Ting Lee,[2] Niran Almudhfar,[2] Mengxi Tian,[2] Andrew Banicki,[2] Marcela Guzmán Ayala,[2] Russell Gordley,[2] Tim K. Lu,[2] Nicholas W. Frankel,[2,*] and Wilson W. Wong[1,3,*]

[1]Department of Biomedical Engineering and Biological Design Center, Boston University, Boston, MA, USA

[2]Senti Biosciences, South San Francisco, CA, USA

[3]Lead contact

*Correspondence: nicholas.frankel@sentibio.com (N.W.F.), wilwong@bu.edu (W.W.W.)

https://doi.org/10.1016/j.cels.2026.101561

SUMMARY

Chimeric antigen receptor (CAR) T cells are powerful cancer immunotherapies, but the lack of tumor-specific single antigens for most cancers limits the therapeutic window. A NOT-gated CAR circuit, consisting of an activating CAR (aCAR) and an inhibitory CAR (iCAR), is particularly powerful because it enables new sets of antigens to be used in tumor targeting. We systematically evaluated more than 60 pairs of NOT-gated CAR circuits. Different inhibitory dose-response characteristics were observed depending on the CD3ζ signaling domain on the aCAR. Furthermore, LIR1-iCAR-expressing T cells display fewer exhaustion phenotypes. Mechanistic studies have shown that SHP-1 is the major intracellular regulator of LIR1-iCAR and the iCAR function in *cis*. Several of the NOT-gated circuits developed in T cells were functionally transferred into primary natural killer (NK) cells. Our NOT-gated CAR circuits provide a precise targeting strategy for safer and more effective cancer immunotherapies.

INTRODUCTION

Chimeric antigen receptor (CAR) T cell therapy has been proven effective against certain hematologic malignancies but has several limitations. In particular, one of the most challenging problems facing CAR T cell therapy, and most cancer therapies in general, is tumor specificity. This problem stems from the lack of unique tumor-specific antigens for most cancers. The specificity issue limits both safety and potency because it can reduce the therapeutic window via dose-limiting toxicity. Another challenge of CAR T cell therapy is its cost. The current method of manufacturing CAR T cells requires using autologous T cells from each patient, which prevents scaling and reduces cost.

Autologous T cells have been the dominant choice of cells to generate CAR-based cellular immunotherapy. However, using an allogeneic cell type would decrease the cost of manufacturing, facilitate quality control, and allow off-the-shelf availability, ultimately increasing access to a broader population. Several allogeneic cell sources have been explored, such as natural killer (NK) cells, gamma delta T cells, NKT cells, and HLA-I and T cell receptor (TCR) deficient T cells.[1–7] Among these choices, allogeneic NK cells expressing CD19 CAR have demonstrated promising clinical results against acute lymphoblastic leukemia (ALL).[1] Furthermore, engineering NK cells is more feasible to achieve clinically adoptable numbers than γδT cells[8,9] and does not require multiple genome editing compared with conventional T cells to prevent graft-versus-host disease.[10–13] Thus, pursuing a highly specific, more cost-effective NK cell therapy for therapeutic purposes is preferable to relying on conventional CAR T cell therapies.

It is widely appreciated that most human cell types, including cancer cells, are best characterized by a *combination* of molecular features. However, existing therapies usually recognize only a single target. Thus, when the chosen targets are "dirty" (i.e., expressed on healthy cells in addition to diseased cells), these existing medicines can generate significant OFF-Target effects. Cell-based therapies are uniquely capable of performing sophisticated logic operations required to discriminate cancer cells specifically. For better discrimination of tumor targeting, both AND-gated[14–20] and NOT-gated[21–30] logic circuits have been engineered in the context of the CAR. Especially with Boolean logic circuits such as these, even more sophisticated strategies for tumor discrimination are possible with AND (A AND B) and NOT-gated (A AND NOT B) CAR circuits by including more target antigens. Notably, including the NOT-gated CAR is indispensable for such combinatorial sensing of multiple antigens, and nearly 70% of the dual-target antigen combinations in the top 10 logic gates per tumor type and over 90% of the triple combinations in the top 100 per tumor type require the presence of NOT-gated CAR.[31]

NOT-gated CAR circuits can be implemented with a dual CAR design consisting of an activating CAR (aCAR) and an inhibitory CAR (iCAR) (Figure 1A). The aCAR[31] targets an antigen found in cancer or healthy cells and activates the CAR T cells, resulting in

Please cite this article in press as: Lee et al., NOT-gated chimeric antigen receptor circuits in T and NK cells, Cell Systems (2026), https://doi.org/10.1016/j.cels.2026.101561

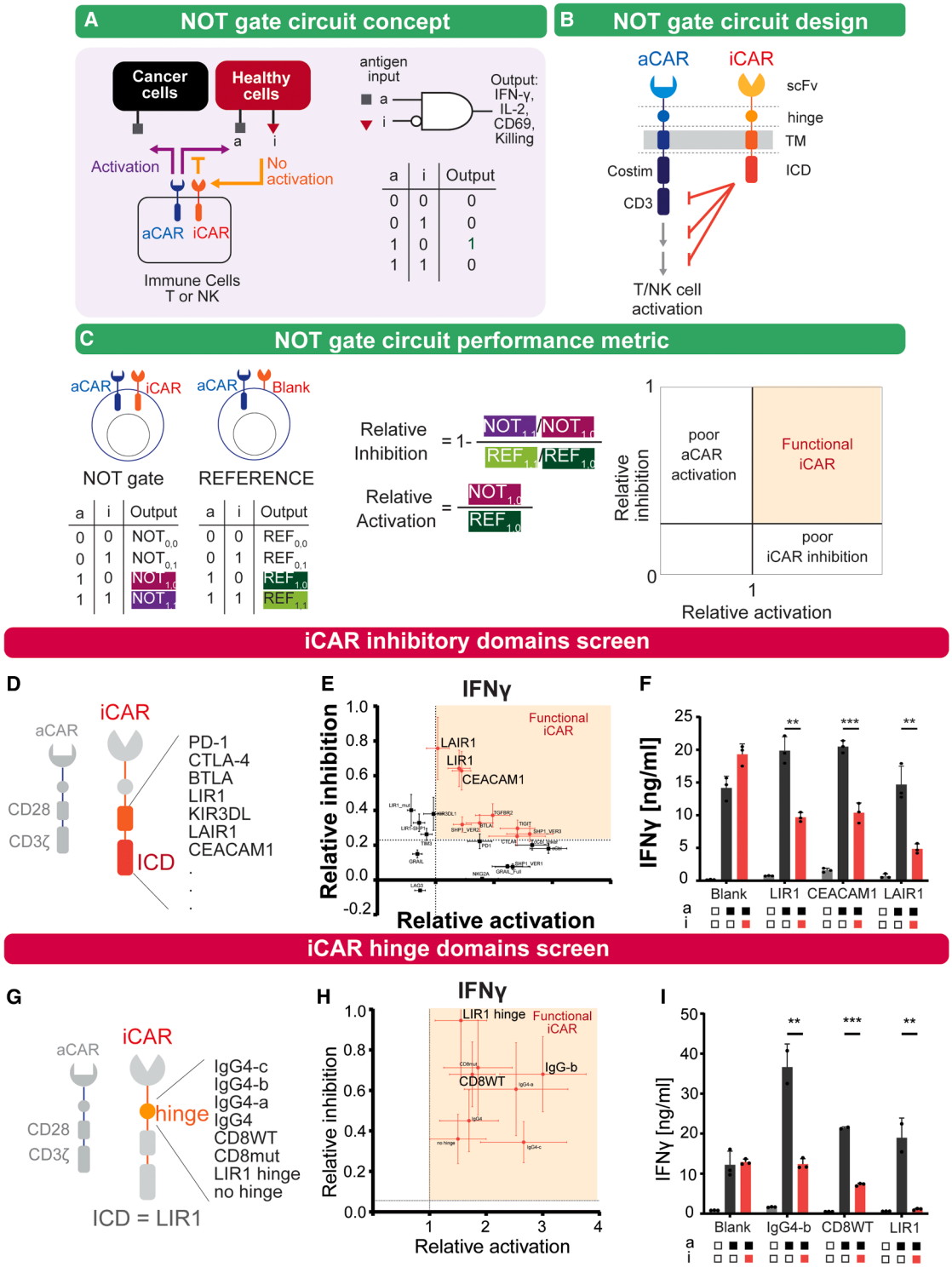

Figure 1. NOT-gate circuit screening strategies and iCAR screening against 28ζ aCAR

(A) Implementation of aCAR and iCAR in the immune cells can distinguish the cancer cells and healthy cells with protective antigen *i*. The inhibition of the immune cell activation by the presence of protective antigen *i* can be measured by several outputs, such as IFNγ, IL-2, CD69, and the target cell killing. The combination of aCAR and iCAR constitutes a NOT-gated CAR circuit detecting *a* AND (NOT *i*) logic, sparing the cells expressing the protective antigen *i*.

(B) NOT-gated CAR circuit can be designed by co-expressing the aCAR and iCAR in the same immune cells. aCAR and iCAR consist of several domains that can be systematically modulated. iCAR functions by inhibiting immune cell activation via aCAR.

(legend continued on next page)

Please cite this article in press as: Lee et al., NOT-gated chimeric antigen receptor circuits in T and NK cells, Cell Systems (2026), https://doi.org/10.1016/j.cels.2026.101561

target cell killing. The iCAR, by contrast, targets a protective antigen only found in healthy cells, thus protecting the healthy cells from the activity of the aCAR. This approach allows for the targeting of antigens that are absent on cancer cells, which is an entirely new class of antigens that have never been used in cancer therapy, opening new opportunities for developing a safe and effective treatment. Since it is less likely that cancer cells will adopt a novel expression of the protective antigen than that they will lose expression of tumor-associated antigens (TAAs), the NOT-gate strategy is safer than the AND gate.

While NOT-gated circuits have been developed previously,[18,21–30] their design space has not been systematically and quantitatively explored, thus preventing us from understanding their design rules. It remains unclear how different inhibitory signaling domains would impact iCAR performance. Furthermore, little is known about how critical structural components of the receptor, such as the hinge and the transmembrane domains, affect the activity of the iCAR.[32–37] Furthermore, the interaction between the aCAR signaling domain and the ability of the iCAR to suppress it has yet to be determined. Lastly, while the NK cell is a promising allogeneic cell type, only two NOT-gated circuits have been reported in primary NK cells,[27] including our recent work on LIR1 iCAR in NK cells, and whether there is a better-performing pair of aCAR and iCAR remains unexplored.

We engineered a collection of aCARs and iCARs by varying their signaling and hinge domains, forming a library of NOT-gated CAR circuits (Figure 1B). We systematically investigated the logic-gating performance of NOT-gated CAR circuits in T cells *in vitro* and *in vivo*. We leveraged several quantitative attribute metrics to systematically compare the performance of different NOT-gated CAR circuits. We also evaluated a number of the NOT gates in NK cells *in vitro* and *in vivo* to determine the portability of the logic CAR circuits into a more promising allogeneic cell type.

RESULTS

To create our iCAR collection, we varied the intracellular signaling and extracellular hinge domains to navigate the functional iCAR candidates (Figure 1B; Table S1). For our aCAR collection, we focused on the costimulatory domain and the CD3 variants. We chose these costimulatory domains because we are interested in understanding how signaling dynamics from the aCAR can impact the inhibitory effect imposed by the iCAR. All the iCAR constructs contained a puromycin-resistant gene after each iCAR domain, including a blank iCAR with no intracellular domain, separated by a P2A ribosome skipping sequence (Figure S1A). To ensure a robust CAR-expressing population, transduced T cells were treated with puromycin 3 days after transduction until the day of screening.

To evaluate our NOT-gated CAR circuits, we challenged them with four different conditions: (1) no antigen; (2) aCAR-specific antigen, *a*, only; (3) iCAR-specific antigen (or protective antigen), *i*, only; and (4) both aCAR and iCAR antigens (*a*, *i*) (Figure 1C, left). For the proof-of-concept of the NOT-gated CAR circuits, the aCAR and iCAR are designed to target Axl and Her2, respectively, throughout this paper unless otherwise noted. To ensure consistency and to minimize the possibility of different target cell lines expressing target antigens at varying levels, the initial screens were performed with purified Axl and Her2 extracellular domain protein bound onto the surface of 96-well plates to stimulate aCAR and iCAR expressed on the T cells. As a control, we compare our NOT-gated CAR circuits to the T cells expressing an aCAR and a blank iCAR without the intracellular inhibitory signaling domain. We refer to T cells transduced with an aCAR and blank iCAR as "reference cells." The output T cell activation levels were measured depending on the presence or absence of target antigens *a* and *i*.

To compare the efficacy of NOT gates, we employed two metrics, relative activation and relative inhibition, to evaluate the CAR T cell activity in response to antigen stimulations (Figure 1C, right). When we plotted the NOT-gate response (e.g., interleukin-2 [IL-2], interferon [IFN]γ, and CD69) based on these two metrics, the best performers should appear in the top right quadrant. The basal level of relative inhibition is defined by the T cells expressing "aCAR only" without the blank iCARs (Figure S1B). The aCAR-only group had a lower output level than "aCAR with blank iCAR" upon exposure against iCAR antigen *i* (i.e., $NOT_{1,1}/NOT_{1,0} < REF_{1,1}/REF_{1,0}$ in Figure 1C for the NOT output from aCAR-only T cells) due to the absence of the iCAR scFv domain. Finally, after evaluating our NOT gates (over 50 pairs of aCAR and iCAR) in T cells, we selected 12 pairs to test in NK cells.

A CAR consists of extracellular, transmembrane, and signaling domains. To generate our iCAR collection for the initial screening of iCAR, we adopted 21 signaling domains from one of the following categories: inhibitory receptors of T cells and NK cells, tyrosine phosphatases, and ubiquitin ligases (Figure 1D). The transmembrane domain was changed in each case to match the signaling domain. The iCARs with 21 different domains were successfully transduced, for which 14, 4, and 3 were from the inhibitory receptors, ubiquitin ligases, and tyrosine phosphatases, respectively. We activated the NOT-gated CAR

(C) NOT-gated CAR circuit performance metric with relative inhibition and relative activation. blank iCAR is adopted as a reference output to match up the effect of iCAR co-transduction on the aCAR expression. Depending on the target antigen expression, there will be four output levels. Relative inhibition is defined as the iCAR specificity, and relative activation is determined by the iCAR-equipped T cell activation level normalized to the reference T cells. The functional iCARs will appear on the top right quadrant of the plots.

(D) iCAR designs with different transmembrane and intracellular signaling domains adopted from native receptors.

(E) iCAR signaling domain screening in IFNγ readout from antigen plate-bound assay. Three highly performing iCAR domains are highlighted.

(F) IFNγ production from T cells with the iCAR domains highlighted in (E). T cells are activated with the indicated antigen below the blot, and all three iCARs can inhibit IFNγ secretion upon iCAR antigen exposure.

(G) LIR1 iCAR designs with different hinge domains, using LIR1 as the signaling domain.

(H) LIR1 iCAR hinge domain screening in IFNγ readout from antigen plate-bound assay. Three representative hinges are highlighted.

(I) IFNγ production from T cells with the LIR1 iCAR hinge domains highlighted in (G). All three iCARs can inhibit IFNγ secretion upon iCAR antigen exposure. For all data presented here, $n = 3$ and error bars represent ± standard deviation. Significance test, Student's *t* test; n.s., not significant; $^{*}p < 0.05$; $^{**}p < 0.01$; $^{***}p < 0.001$.

Please cite this article in press as: Lee et al., NOT-gated chimeric antigen receptor circuits in T and NK cells, Cell Systems (2026), https://doi.org/10.1016/j.cels.2026.101561

T cells with plate-bound antigens and measured IFNγ, CD69, and IL-2 expression from the activated T cells (Figures 1E, 1F, and S1C–S1F). Among the screened domains, LIR1, LAIR1, and CEACAM1 showed the highest relative inhibition in the three activation markers.

Next, we explored whether variation in hinge domains of the iCAR affects inhibitory function (Figure 1G). Based on its high NOT-gate performance, we first chose to use LIR1 for the transmembrane and intracellular domains. We screened nine hinge domains from other published aCAR papers or inhibitory receptors.[17,36,38–42] Among them, the LIR1 hinge outperformed in relative inhibition compared with other hinge domains (Figures 1H and 1I). Although the distinction between the rest of the hinge variations was not as distinctive as among the domain variations, we determined that the CD8WT hinge and IgG4CH2mutCH3 hinge (labeled as IgG4-b in the figure) were the next high-ranked in CD69 (Figures S2A and S2B) and IL-2 readout (Figures S2C and S2D). The high relative inhibition of the IgG4CH2mutCH3 hinge resulted from increased activation against the aCAR antigen, *a*, although the IFNγ and IL-2 secretion level against the iCAR antigen, *i*, was similar to that of the blank iCAR (Figures 1I, S2B, and S2D). We also explored transmembrane domain variation of CD8WT hinge LIR1 iCAR, comparing LIR1TM with CD28TM (also used in the aCAR), expecting that the swap may cause a stronger interaction between the aCAR and iCARs[37] (Figures S2E–S2G), but observed the opposite result. Hinge variations on other domains were also explored with CEACAM1 and LAIR1 domains (data not shown). In both cases, the CD8WT hinge resulted in the best performance. The protection against OFF-Tumor cells expressing the protective antigen was less than 20% from the initial killing assay, so we did not further investigate CEACAM1- and LAIR1-based iCAR in T cells.

To evaluate the performance of an LIR1 iCAR in suppressing different aCARs, we first paired the iCAR with 1st, 2nd, and 3rd generation aCARs (Figure 2A). The intracellular domain of the 1st generation CAR consisted of a CD3ζ domain alone. The 2nd generation adds either CD28 or 4-1BB costimulatory domains. The 3rd generation has both CD28 and 4-1BB costimulatory domains with CD3ζ. NOT-gated CAR circuit containing a aCAR with a CD28 costimulatory domain showed the most robust inhibition of IL-2 (Figures 2B and 2C), CD69, and IFNγ responses (Figures S3A and S3B). LIR1 iCAR could inhibit 1st-generation aCAR-mediated CD69 expression and IFNγ secretion, but not IL-2 secretion (Figures 2B and 2C). The NOT gate consisting of an aCAR with a 4-1BB costimulatory domain paired with an LIR1 iCAR showed weak relative activation (<1), suggesting a potential basal inhibitory effect of LIR1 iCAR on this aCAR. To better evaluate the overall performance of the NOT-gate CAR circuits across all readouts, we developed an attribute diagram based on normalized relative inhibition and relative activation level (Figure 2D). This attribute diagram has four vertices, each representing CD69, IL-2, IFNγ, and cell killing measurement. The distance from the center to the vertex represents either relative inhibition (red) or relative activation (black), normalized to the maximum level observed among the four aCAR/LIR1 iCAR pairs. As shown from the attribute diagrams (Figure 2E), aCAR with the CD28 costimulatory domain alone has the largest area and therefore was chosen for further development.

With the costimulatory domain on the aCAR optimized, we further determined if any modifications to the CD3ζ chain can enhance the activation and inhibition profile. CD3ζ has three immunotyrosine activation motifs (ITAMs), and the combination with a costimulatory domain may provide excessive and redundant signaling that can lead to T cell dysfunction and exhaustion.[43–45] We hypothesized that with a more refined CD3ζ signaling, we might identify an optimal pair for the NOT-gated CAR circuit. We adopted three aCAR variations of the CD3ζ activation domain in addition to the original 28ζ: mutation on the second and third ITAM as 28ζ(D23), deletion of the second and third ITAM as 28ζ(1XX), or additional CD3ε domain as CD3ε-28ζ (Figure S3C).[43,46] From plate-bound stimulation assays, 28ζ(D23) aCAR showed the highest relative inhibition and relative activation in IL-2 secretion (Figures S3C and S3D) and CD69 expression (Figures S3E and S3F). However, distinguishing the performance in terms of IFNγ secretion was challenging, as all four aCARs clustered together on the relative inhibition and relative activation plot higher than 1. Notably, all three 28ζ aCAR variants showed slightly better relative inhibition performance than the conventional 28ζ aCAR (Figure S3G).

We next determined whether different CD3ζ variants have distinct antigen dose-response profiles. Across a range of antigen dosages, aCAR with the intracellular domain of 28ζ (Figure 3A), 28ζ(1XX) (Figure 3B), and CD3ε-28ζ (Figure 3C) paired with LIR1 iCAR showed a similar pattern for the activation and inhibition in the CD69 readout. By contrast, 28ζ(D23) with LIR1 iCAR displayed a more step-like profile in activation and inhibition, with aCAR-mediated activation increasing steeply from 100 to 500 ng of aCAR antigen, and iCAR-mediated inhibition dropping activation similarly steeply to the basal level from 20 to 100 ng of iCAR antigen (Figure 3D). The high-sensitivity response to iCAR antigen was even more distinct at the highest aCAR antigen dosage (Figure S4A).

The original 28ζ aCAR paired with LIR1 iCAR (Figures 3E and 3F) exhibited robust inhibition of killing of OFF-Tumor Nalm6 cells, but only at a low E:T ratio (1:4). By contrast, the 28ζ(D23) variant showed robust inhibition in killing, even in a high E:T ratio of 1:1, and ∼50% of the killing was inhibited against the OFF-Tumor Nalm6 cells (Figures 3G and 3H). Both the 28ζ and 28ζ(D23) variants exhibited similar cytotoxicity against ON-Tumor Nalm6 cell killing when paired with either the LIR1 iCAR or blank iCAR. The cytotoxicity against OFF-Tumor Nalm6 cells by the 28ζ(1XX) aCAR variant could also be inhibited by the LIR1 iCAR at a low E:T ratio of 1:4 but not at the higher E:T = 1:1 and 1:2 (Figures S4B and S4C). The CD3ε-28ζ aCAR variant was also successfully inhibited by the LIR1 iCAR (Figures S4D and S4E). However, both 28ζ(1XX) and CD3ε-28ζ aCAR variants with the LIR1 iCAR showed decreased killing against ON-Tumor Nalm6 cells compared with the blank iCAR pair (Figures S4B and S4D). By contrast, such an effect was not as significant in the 28ζ or 28ζ(D23) aCAR variant (Figures 3E and 3G).

After characterizing the NOT-gated CAR circuits *in vitro*, we investigated the LIR1 protection effect against OFF-Tumor Nalm6 cells expressing the protective antigen Her2 in a mouse xenograft tumor model (Figure 4A). We wanted to verify that the LIR1 iCAR can protect against the killing of ON-Tumor target cells even when OFF-Tumor cells are present within the same animal. As such, we developed a dual-target cell model where both the

Please cite this article in press as: Lee et al., NOT-gated chimeric antigen receptor circuits in T and NK cells, Cell Systems (2026), https://doi.org/10.1016/j.cels.2026.101561

CellPress

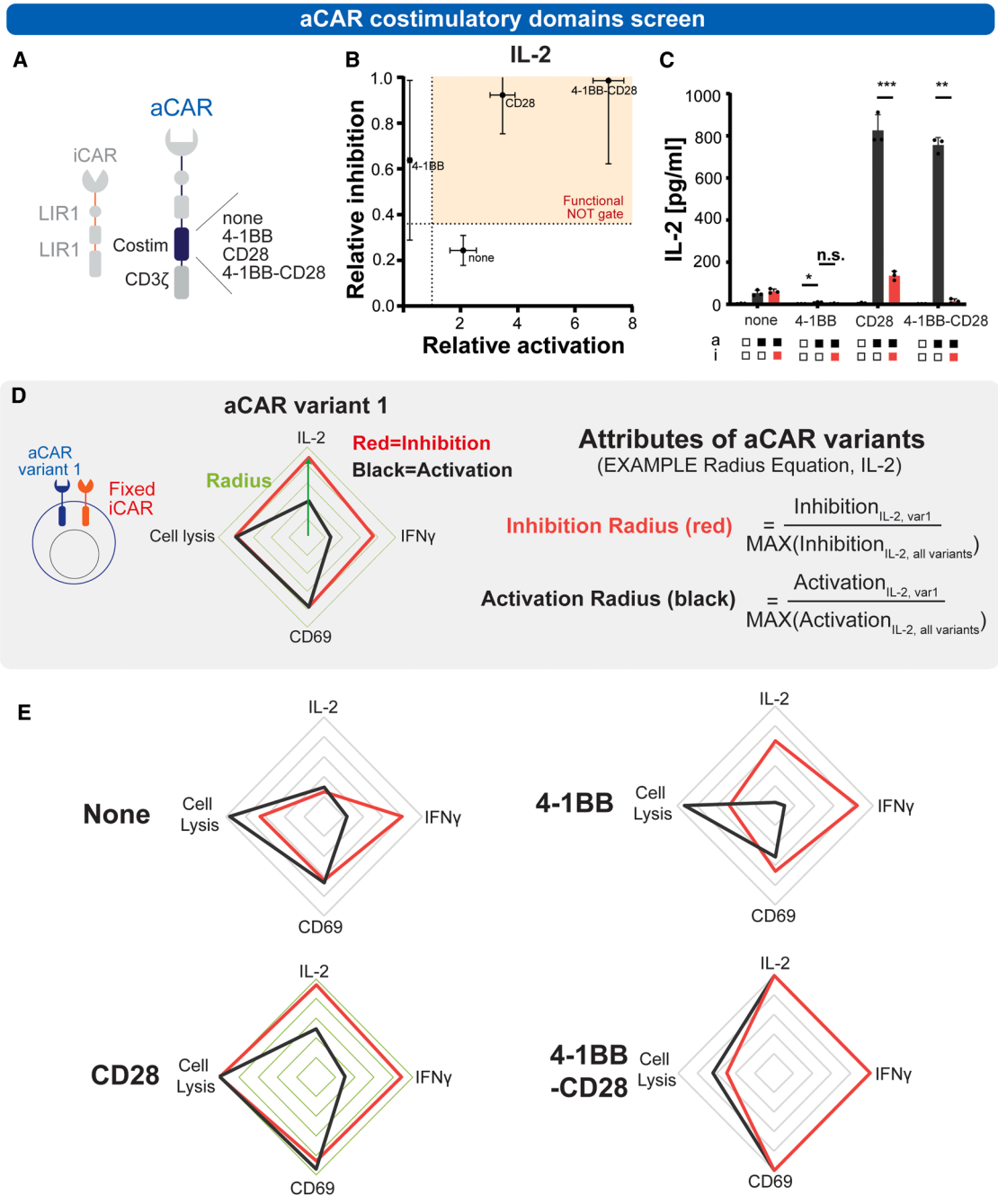

Figure 2. aCAR costimulatory domains screening

(A) NOT-gated circuit screening with various aCAR costimulatory domains, using LIR1 hinge LIR1 iCAR. Only costimulatory domains were changed, while other domains remained the same.

(B) aCAR costimulatory domain screening with IL-2 readout from antigen plate-bound assay. CD28 and 4-1BB-CD28 costimulatory domains performed well.

(C) IL-2 secretion data from the plate-bound assay in (B). aCAR with CD28 and 4-1BB-CD28 costimulatory domain can inhibit the IL-2 secretion in the presence of the iCAR antigen *i*.

(D) aCAR variant evaluation strategy from four output parameters: IL-2, IFNγ, CD69, and target cell lysis. The inhibition radius, labeled as red, is normalized to the maximum relative inhibition observed in all aCAR variants, and the activation radius, labeled as black, is normalized to the maximum relative activation observed. The radius in cell lysis has been calculated from the ON-Tumor killing (for activation radius) and OFF-Tumor killing protection (for inhibition) percentage average in 3 different E:T ratios.

(E) aCAR costimulatory variant evaluation based on the attributes explained in (D). aCAR with a CD28 costimulatory domain has been selected for further experiment in T cells, which is highlighted in green. For all data presented here, $n = 3$ and error bars represent ± standard deviation. Significance test, Student's *t* test; n.s., not significant; $^{*}p < 0.05$; $^{**}p < 0.01$; $^{***}p < 0.001$.

Please cite this article in press as: Lee et al., NOT-gated chimeric antigen receptor circuits in T and NK cells, Cell Systems (2026), https://doi.org/10.1016/j.cels.2026.101561

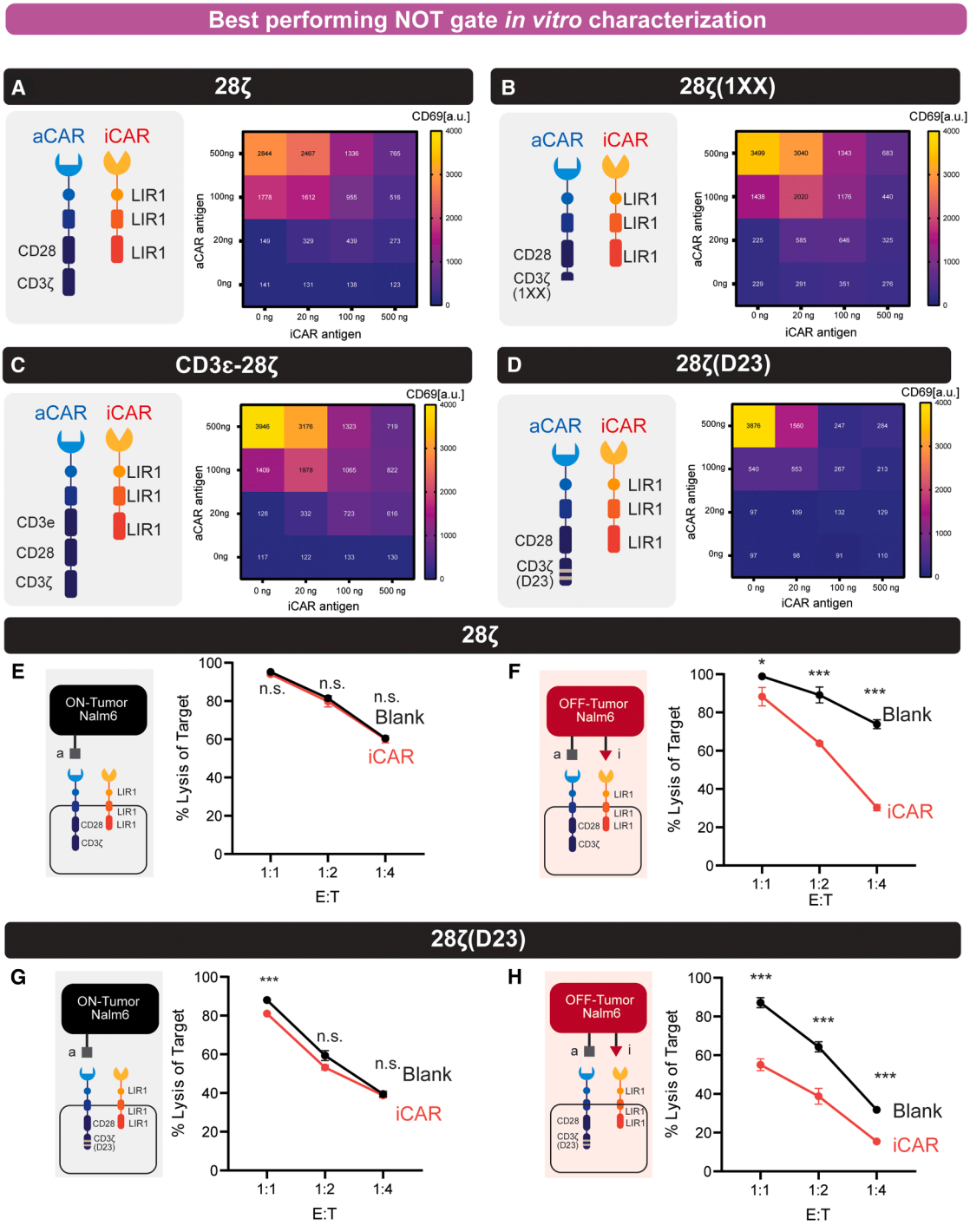

Figure 3. NOT-gate circuit profile in vitro characterization

CD69 expression level (24 h post incubation) of (A) 28ζ, (B) 28ζ(1XX), (C) CD3ε-28ζ, and (D) 28ζ(D23) aCAR with LIR1 iCAR, co-transduced into T cells and activated with plate-bound antigens at the indicated dosage.

(E and F) 28ζ aCAR + LIR1 hinge LIR1 iCAR-equipped T cell killing against ON-Tumor Nalm6 cells expressing aCAR target antigen Axl in (E) and killing against OFF-Tumor Nalm6 cells expressing aCAR target antigen Axl and iCAR target antigen Her2 in (F). Blank and the LIR1 iCAR-equipped T cells did not show significant differences in killing against ON-Tumor Nalm6 cells, but LIR1 iCAR-equipped T cells showed significantly decreased target lysis against OFF-Tumor Nalm6 cells.

(G and H) 28ζ(D23) aCAR + LIR1 hinge LIR1 iCAR-equipped T cell killing against ON-Tumor Nalm6 cells expressing aCAR target antigen Axl in (G) and killing against OFF-Tumor Nalm6 cells expressing aCAR target antigen Axl and iCAR target antigen Her2 in (H). Blank and the LIR1 iCAR-equipped T cells did not show significant differences in killing against ON-Tumor Nalm6 cells, but LIR1 iCAR-equipped T cells showed significantly decreased target lysis against OFF-Tumor Nalm6 cells. For all data presented here, $n = 3$ and error bars represent ± standard deviation. Significance test, Student's t test; n.s., not significant; $^{*}p < 0.05$; $^{**}p < 0.01$; $^{***}p < 0.001$.

Please cite this article in press as: Lee et al., NOT-gated chimeric antigen receptor circuits in T and NK cells, Cell Systems (2026), https://doi.org/10.1016/j.cels.2026.101561

CellPress

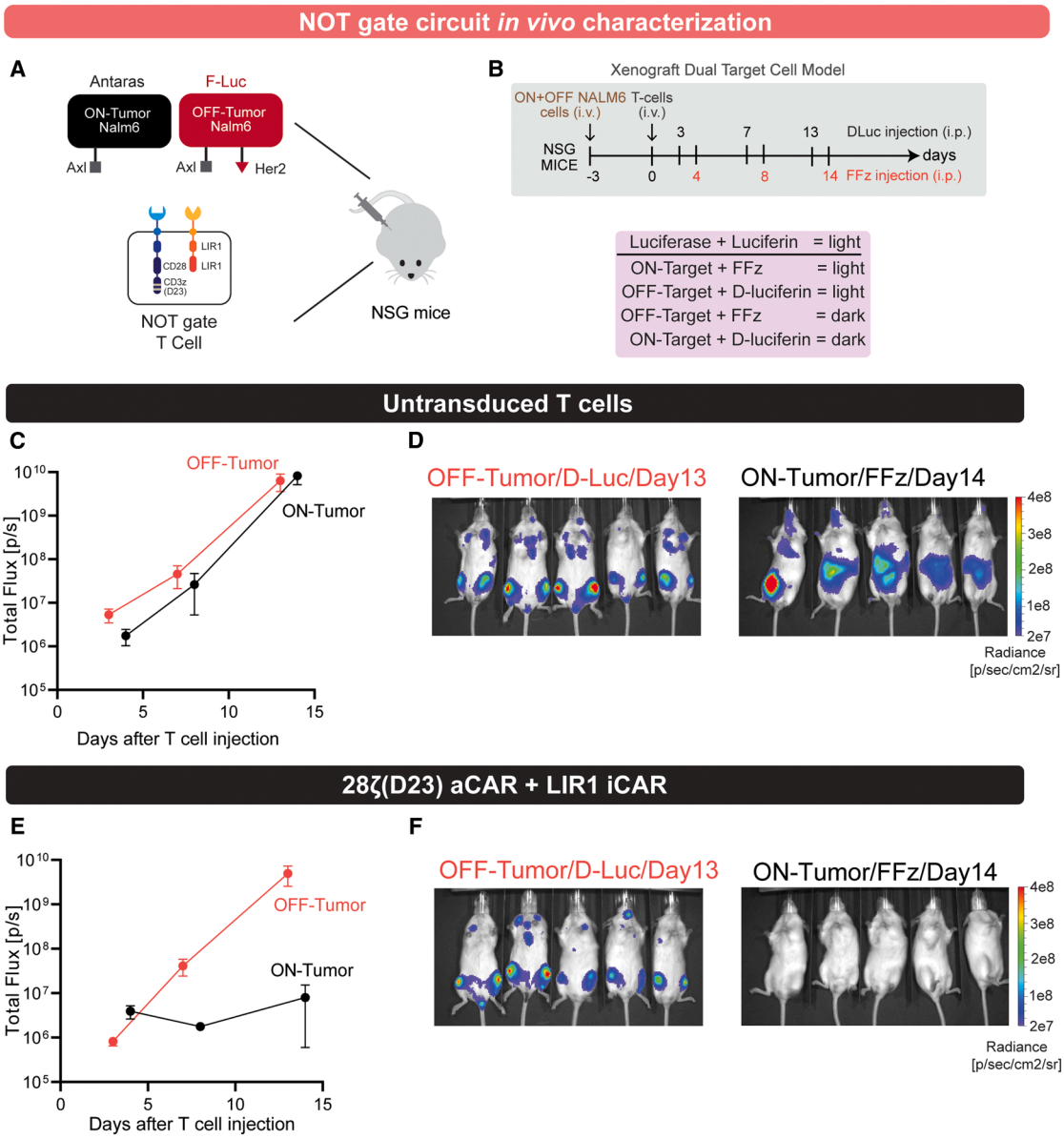

Figure 4. NOT-gate circuit in vivo characterization

(A) Dual tumor xenograft mouse model. ON-Tumor Nalm6 cells express Axl and can be detected with Antares activity. OFF-Tumor Nalm6 cells express Axl and Her2 and can be detected with F-Luc activity.

(B) ON-Tumor and OFF-Tumor Nalm6 were injected intravenously on the same day, and the T cells were injected intravenously 4 days after tumor injection. ON-Tumor and OFF-Tumor Nalm6 encoding two orthogonal luciferases were distinctively measured with different substrates: F-Luc with D-luciferin and Antares with Fluorofurimazine (FFz). There was a 24-h gap between each substrate injection to ensure the degradation of D-luciferin before FFz injection.

(C) Tumor luminescence measured from the group treated with untransduced T cells. The two tumor burdens expressing two different luciferases were measured with a 1-day stagger. Untransduced T cells did not show any discrepancy in OFF-Tumor and ON-Tumor elimination.

(D) Luminescent images of the mouse group treated with untransduced T cells after the dual tumor injection.

(E) Tumor luminescence measured from the group treated with 28ζ aCAR with LIR1 iCAR co-transduced T cells. The two tumor burdens expressing two different luciferases were measured with a 1-day stagger. 28ζ aCAR with LIR1 iCAR co-transduced T cells decreased ON-Tumor burden while sparing the OFF-Tumor burden.

(F) Luminescent images of the mouse group treated with 28ζ aCAR/LIR1 iCAR co-transduced T cells after the dual tumor injection. For all data presented here, $n = 5$ and error bars represent ± standard deviation. Significance test, Student's t test; n.s., not significant; $^{*}p < 0.05$; $^{**}p < 0.01$; $^{***}p < 0.001$.

ON- and OFF-Tumor cells are present in the same mice. We engineered the OFF-Tumor and ON-Tumor Nalm6 cells to express two orthogonal luminescence reporters, firefly luciferase (F-Luc) and Antares, respectively.[47] F-Luc uses D-luciferin, and Antares requires fluorofurimazine (FFz) as the substrate via independent mechanisms, and they have been used to track two different cell types *in vivo* previously.[47–49] We inject both cell lines into NOD.Cg-Prkdcscid Il2rgtm1Wjl/SzJ (NSG) mice intravenously

Please cite this article in press as: Lee et al., NOT-gated chimeric antigen receptor circuits in T and NK cells, Cell Systems (2026), https://doi.org/10.1016/j.cels.2026.101561

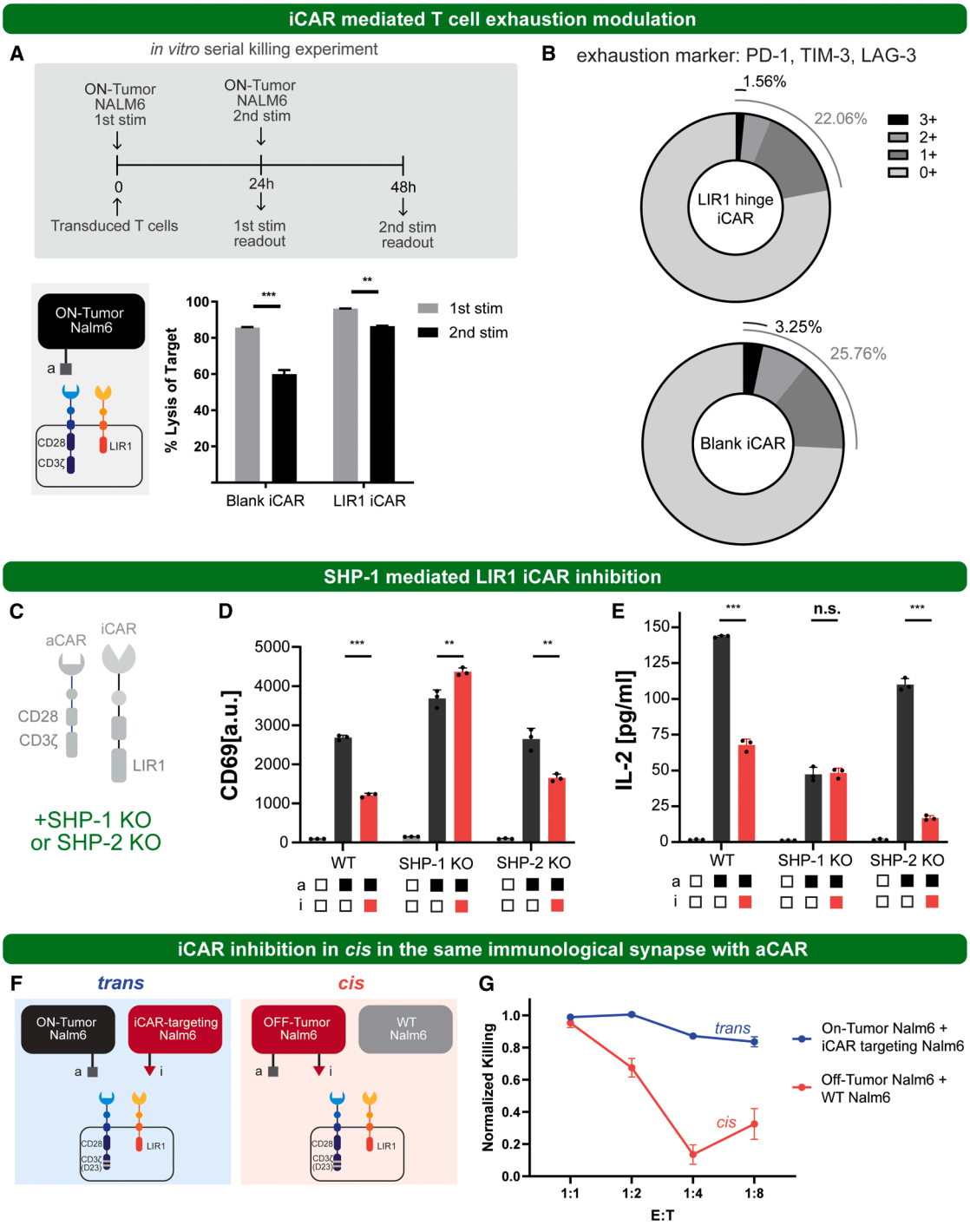

Figure 5. Modulation of T cell exhaustion and inhibition mechanisms in iCAR

(A) Repetitive stimulation of the T cells transduced with 28ζ aCAR with blank iCAR or LIR1 iCAR. T cells were stimulated with ON-Tumor Nalm6 with a 24-h gap, and target cell killing was measured at 24 and 48 h after first stimulation. 28ζ aCAR with blank iCAR showed a higher decrease in killing on the second stimulation compared with the 28ζ aCAR with LIR1 iCAR.

(B) Exhaustion markers were measured in T cells transduced with 28ζ aCAR and indicated iCARs. PD-1, TIM-3, and LAG-3 were stained 10 days after the transduction. Triple-positive and single-positive populations were higher at the T cells transduced with 28ζ aCAR with Blank iCAR.

(C) SHP-1 or SHP-2 KO Jurkat cell lines were transduced with anti-ROR1 28ζ aCAR and LIR1 iCAR and assessed with a plate-bound assay with ROR1 as antigen *a* and Her2 as antigen *i*.

(D) CD69 expression on the Jurkat cells from (C) in the plate-bound assay. SHP-1 KO Jurkat cells transduced with anti-ROR1 28ζ aCAR and LIR1 iCAR showed higher CD69 expression.

(E) IL2 secretion from the Jurkat cells from (C) in the plate-bound assay. SHP-1 KO ameliorated the LIR1-mediated inhibition of IL-2 secretion, but not SHP-2.

(legend continued on next page)

3 days before the injection of T cells. The luminescence from each luciferase was measured 1 day apart to ensure full decay of the F-Luc signal before Antares measurement (Figure 4B). While untransduced T cells did not lead to any differential killing between OFF-Tumor and ON-Tumor cells (Figure 4C) nor did the 28ζ(D23) aCAR + blank iCAR transduced T cells (Figures S4F and S4G), the 28ζ(D23) aCAR + LIR1 iCAR NOT-gated CAR T cells showed discriminative killing between OFF- and ON-Tumor Nalm6 cells (Figure 4E). LIR1 iCAR and Blank iCAR have similar transduction efficiencies (Figure S4F). (The NOT-gated CAR T cells killed ON-Tumor cells significantly while sparing the OFF-Tumor cell killing.

Although we observed complete remission with 28ζ(D23) aCAR + LIR1 iCAR NOT-gated CAR T cells *in vivo* (Figure 4E), 28ζ(D23) aCAR + blank iCAR transduced T cells did not result in the complete elimination of the tumor (Figures S4F and S4G). The expression of aCAR levels on the day of injection was within 2% variance (data not shown), so we hypothesized that adding the LIR1 domain could ameliorate the exhaustion of the T cells. We performed a serial stimulation of the T cells with the ON-Tumor Nalm6 cells and measured the cytotoxicity changes in the two serial stimulations (Figure 5A). Killing against the ON-Tumor Nalm6 has been maintained with 28ζ aCAR + LIR1 iCAR transduced T cells but not with 28ζ aCAR + blank iCAR transduced T cells. The Blank iCAR containing T cells had more than a 20% cytotoxicity decrease against both ON-Tumor. Representative exhaustion markers were measured on the transduced T cells with 28ζ aCAR and indicated iCAR (Figure 5B). Compared with blank iCAR, LIR1 hinge LIR iCAR showed fewer triple-positive markers, which indicates less exhaustion.

To identify the mechanism of iCAR further, we selected SHP-1 and SHP-2 inhibitory phosphatases[50,51] as the potential proteins mediating the signal of iCAR. We received SHP-1 or SHP-2 knockout (KO) Jurkat cell line as a gift from the Enfu Hui Lab (UCSD) and transduced the 28ζ aCAR and LIR1 iCAR (Figure 5C). Upon exposure to the aCAR and iCAR antigens, LIR1 iCAR could suppress the activation in wild-type (WT) Jurkat cells and SHP-2 KO Jurkat cells, but not in the SHP-1 KO Jurkat cell line (Figures 5D and 5E). We speculate that SHP-1 can be the major regulator of the LIR1 iCAR-mediated inhibition. We then investigated whether the iCAR functions in *cis* or *trans*. To test each hypothesis, we conducted a co-culture experiment comparing the killing activity of 28ζ aCAR + LIR1 iCAR versus 28ζ aCAR + blank iCAR. For the *trans* hypothesis, the target cells consisted of ON-Target cells and iCAR antigen-expressing target cells. For the *cis* hypothesis, the target cells included OFF-target tumor cells and WT Nalm6 cells (Figure 5F). If the LIR1 iCAR functions in *trans*, T cells transduced with 28ζ aCAR + LIR1 iCAR should exhibit increased inhibition of ON-Target cells compared with those transduced with 28ζ aCAR + blank iCAR. Conversely, if the mechanism is cis-dependent, the observed inhibition would arise exclusively from OFF-Tumor cells expressing both aCAR and iCAR antigens. The killing against aCAR antigen *a* expressing Nalm6 (either ON-Tumor or OFF-Tumor cells) observed from the 28ζ aCAR + LIR1 iCAR was normalized to the killing from 28ζ aCAR + blank iCAR (Figure 5G). The effect of the trans mechanism was minimal when targeting Nalm6 with iCAR, in comparison to the cis mechanism.

Unlike T cells, NK cells are known to be resistant to virus-mediated gene delivery, and they are more challenging to culture than T cells.[52–54] We decided to narrow down the NOT-gated CAR candidates from T cells to facilitate the identification of functional NOT-gated CAR circuits in NK cells. We selected LIR1, LAIR1, CEACAM1, and KIR3DL1 iCARs, which were highly inhibitory in the iCAR screening from T cells. We also included a PD-1 iCAR that was previously reported to be inhibitory in the NK-92 cell line.[55] Each iCAR was paired with a 28ζ aCAR, and the killing assay was set up against the ON- and OFF-Tumor Nalm6 cells (Figure 6A). As expected, while the 28ζ-blank iCAR did not show any differences in cytotoxicity against ON-Tumor and OFF-Tumor, iCARs with LIR1, LAIR1, and CEACAM1 domains showed diminished killing against OFF-Tumor cells compared with the ON-Tumor killing (Figures 6B and 6C). In contrast to prior reports,[25,55] the PD-1 iCAR did not show any better inhibition against OFF-Tumor cells. However, all the iCARs showed statistically significant inhibition of tumor necrosis factor α (TNF-α) and IFNγ secretion (Figures S5A–S5D). The LIR1 iCAR showed the best protection against OFF-Tumor cells, so we further investigated by varying the hinge domain to determine if the effect was similar to what we observed in T cells (Figure 6D). The best hinge for LIR1 iCAR in the context of NK cells was the CD8WT hinge and the IgG4CH2CH3mut (labeled as IgG4-b) hinge (Figures 6E and 6F). We further characterized the cytotoxicity of those two iCARs paired with 28ζ aCAR at different E:T ratios. The best protection of OFF-Tumor was observed with the CD8WT hinge LIR1 iCAR (Figures 6G and 6H). The IgG4CH2CH3mut hinge LIR1 iCAR also showed significantly less cytotoxicity against OFF-Tumor killing (Figures S5E and S5F). Since this construct created a large payload size that may hinder the transduction, we decided to proceed with the CD8WT hinge for the *in vivo* study. We also tested if the 28ζ(D23) aCAR can be utilized in primary NK cells (Figure S5G), but it showed weaker activity than 28ζ aCAR against ON-Tumor cells.

Lastly, we validated the NOT-gate CAR circuit in primary NK cells *in vivo*. We first leverage a separate xenograft mouse model by injecting ON-Tumor and OFF-Tumor cells in a different set of mice, followed by the NOT-gated CAR NK cell injection (Figure 7A). Tumor growth was monitored every 3–4 days by bioluminescence imaging of firefly luciferase expressed by both ON- and OFF-Tumor Nalm6 cells (Figure 7B). Both aCAR-only and aCAR + iCAR NOT-gated CAR NK cells were able to

(F) Tri co-culture set-up with different target cells to test in *cis* and in *trans* hypotheses. To observe any effect from in *trans* inhibition, ON-Tumor Nalm6 expressing antigen *a* as Axl and iCAR-targeting Nalm6 expressing antigen *i* as Her2 were seeded at an ON-Tumor Nalm6: iCAR-targeting Nalm6 = 1:4 ratio. To test in *cis* inhibition effect, OFF-Tumor Nalm6 expressing antigen *a* and antigen *i* and WT Nalm6 were seeded at OFF-Tumor Nalm6:WT Nalm6 = 1:4 ratio.

(G) T cells transduced with 28ζ(D23) aCAR and LIR1 iCAR were co-cultured with the target cells from (F) at the E:T ratio as noted on the graph, and the killing of antigen *a*-expressing target cells (*trans*: ON-Tumor Nalm6; *cis*: OFF-Tumor Nalm6) was normalized to the killing from the T cells transduced with 28ζ(D23) aCAR and blank iCAR at the same setup. *In trans* effect was minimal compared with the *in cis* effect. For all data presented here, $n = 3$ and error bars represent ± standard deviation. Significance test, Student's *t* test; n.s., not significant; $^{*}p < 0.05$; $^{**}p < 0.01$; $^{***}p < 0.001$..

Please cite this article in press as: Lee et al., NOT-gated chimeric antigen receptor circuits in T and NK cells, Cell Systems (2026), https://doi.org/10.1016/j.cels.2026.101561

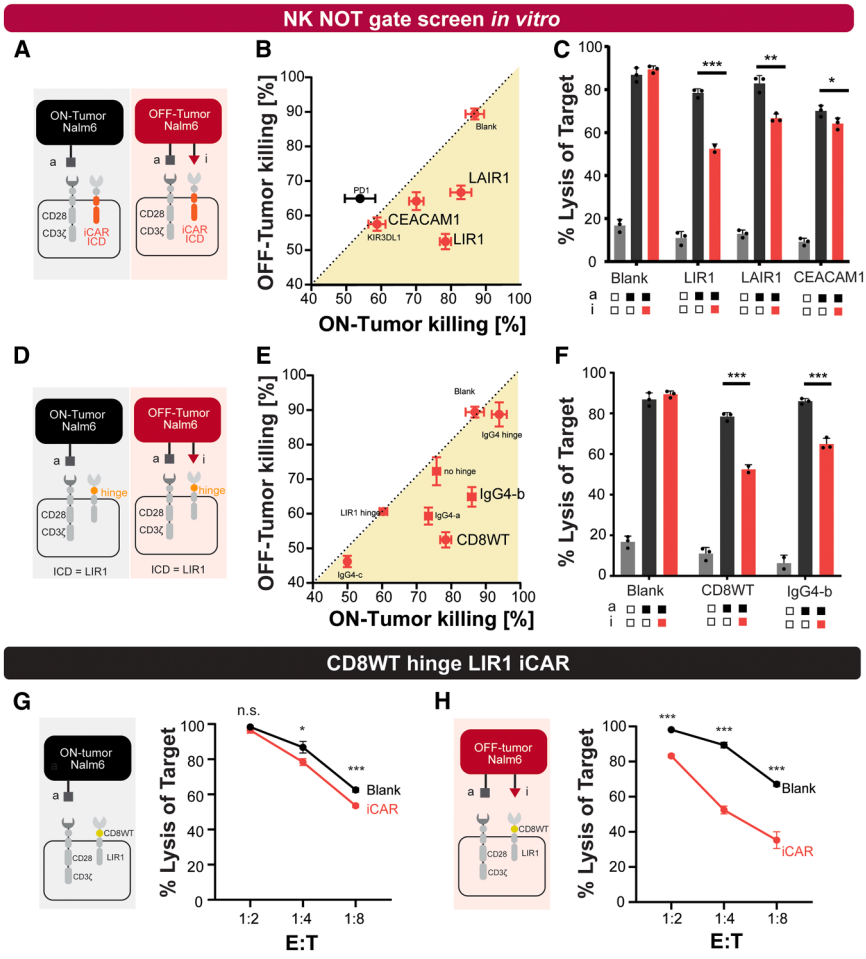

Figure 6. NOT-gate circuit screen in vitro in primary NK cells

(A) Schematics of the iCAR screening with intracellular domain (ICD) variation in NK cells with 28ζ aCAR against ON-Tumor and OFF-Tumor Nalm6. The aCAR antigen *a* is Axl, and the iCAR antigen *i* is Her2.

(B) ON-Tumor-killing and OFF-Tumor-killing ability assessed for each ICD domain screened in NK cells. Blank iCAR did not show a discrepancy between killing ON-Tumor and OFF-Tumor, whereas LIR1, LAIR1, and CEACAM1 iCAR showed less OFF-Tumor killing than ON-Tumor killing.

(C) Lysis of each target cell was measured 24 h after the co-culture with NK cells equipped with the indicated iCAR. WT Nalm6 cells do not express any aCAR or iCAR target antigens; ON-Tumor Nalm6 cells express antigen *a* as Axl, and OFF-Tumor Nalm6 cells express antigen *i* as Her2.

(D) Schematics of the iCAR screening with hinge domain variation in NK cells with 28ζ aCAR against ON-Tumor and OFF-Tumor Nalm6 cells. aCAR antigen *a* is Axl, and iCAR antigen *i* is Her2. The ICD domain has been fixed to LIR1 ICD.

(E) ON-Tumor killing and OFF-Tumor killing ability assessed for each hinge domain screened in NK cells. CD8WT hinge, IgG4-b hinge LIR1 iCAR is highlighted, which showed the highest OFF-Tumor protection.

(F) Lysis of each target cell was measured 24 h after the co-culture with NK cells equipped with indicated hinge-varied LIR1 iCAR.

(G) 28ζ aCAR + CD8WT hinge LIR1 iCAR NOT-gated CAR-NK cell killing against ON-Tumor Nalm6 cells. Blank and the LIR1 iCAR did not show significant differences in killing against ON-Tumor Nalm6 cells.

(H) 28ζ aCAR + CD8WT hinge LIR1 iCAR NOT-gated CAR NK cell killing against OFF-Tumor Nalm6 cells. 28ζ-CD8WT hinge LIR1 iCAR-equipped NK cells showed less killing of OFF-Tumor Nalm6 cells than the NK cells with blank iCAR. For all data presented here, $n = 3$ and error bars represent ± standard deviation. Significance test, Student's *t* test; n.s., not significant; $^{*}p < 0.05$; $^{**}p < 0.01$; $^{***}p < 0.001$.

hinder the ON-Tumor growth (Figure 7C). Only the NOT-gated CAR NK cells exhibited less cytotoxicity against OFF-Tumor cells, demonstrating NOT-gate function *in vivo* (Figure 7D).

We also evaluated the *in vivo* performance in a dual-target cell xenograft mouse model (Figure 7E). The ON- and OFF-Tumor cells were injected simultaneously, followed by NK cell injection. Peripheral blood samples were collected 14 days after the NK cell injection (Figure 7F). We measured target cell counts of both ON- and OFF-Tumor cells from mice injected with either aCAR only or aCAR + iCAR NOT-gated CAR NK cells, then normalized the cell reduction relative to the blood sample from mice treated with PBS only (no NK cells) (Figure 7G). Cell counts were normalized to the volume of the blood sample. While 28ζ aCAR transduced NK cells did not show any difference in the killing against ON-Tumor and OFF-Tumor cells, 28ζ aCAR + LIR1 iCAR NOT-gated CAR NK cells showed significantly less killing against OFF-Tumor cells relative to the ON-Tumor cells. Such an effect was also evident in the frequency of target cells relative to $CD45^{+}$ cells (Figure S5H). When we measured the OFF-Tumor population among the tumor cells collected from the mice, 28ζ aCAR + LIR1 iCAR NOT-gated CAR NK-cell-injected mice had a significantly higher population of the OFF-Tumor cells compared with both PBS-treated and the 28ζ aCAR transduced NK cell-treated mice (Figure 7H). Altogether, we demonstrated that NOT-gated CAR NK cells could kill the ON-Tumor population while preserving the OFF-Tumor population *in vivo*.

DISCUSSION

In this work, we systematically explored the NOT-gated CAR circuit design space, including the design features from both aCARs and iCARs. We found that iCARs with LIR1, LAIR1, and CEACAM1 intracellular signaling domains have the most potent inhibitory function. The robustness of LIR1-based iCAR, in particular, has been independently corroborated by others.[23,26] Interestingly, the most well-known checkpoint receptors (e.g., PD-1, LAG3, and TIM3) are not the top iCAR performers. Furthermore, recent innovative aCAR screens and designs[56,57] also uncovered intracellular signaling domains that are outside of the canonical TCR/4-1BB/CD28 signaling paradigm. Together, these results highlight the different roles that checkpoint receptors and immune stimulatory can have in synthetic receptor design for anti-cancer vs. normal physiological function.

Please cite this article in press as: Lee et al., NOT-gated chimeric antigen receptor circuits in T and NK cells, Cell Systems (2026), https://doi.org/10.1016/j.cels.2026.101561

CellPress

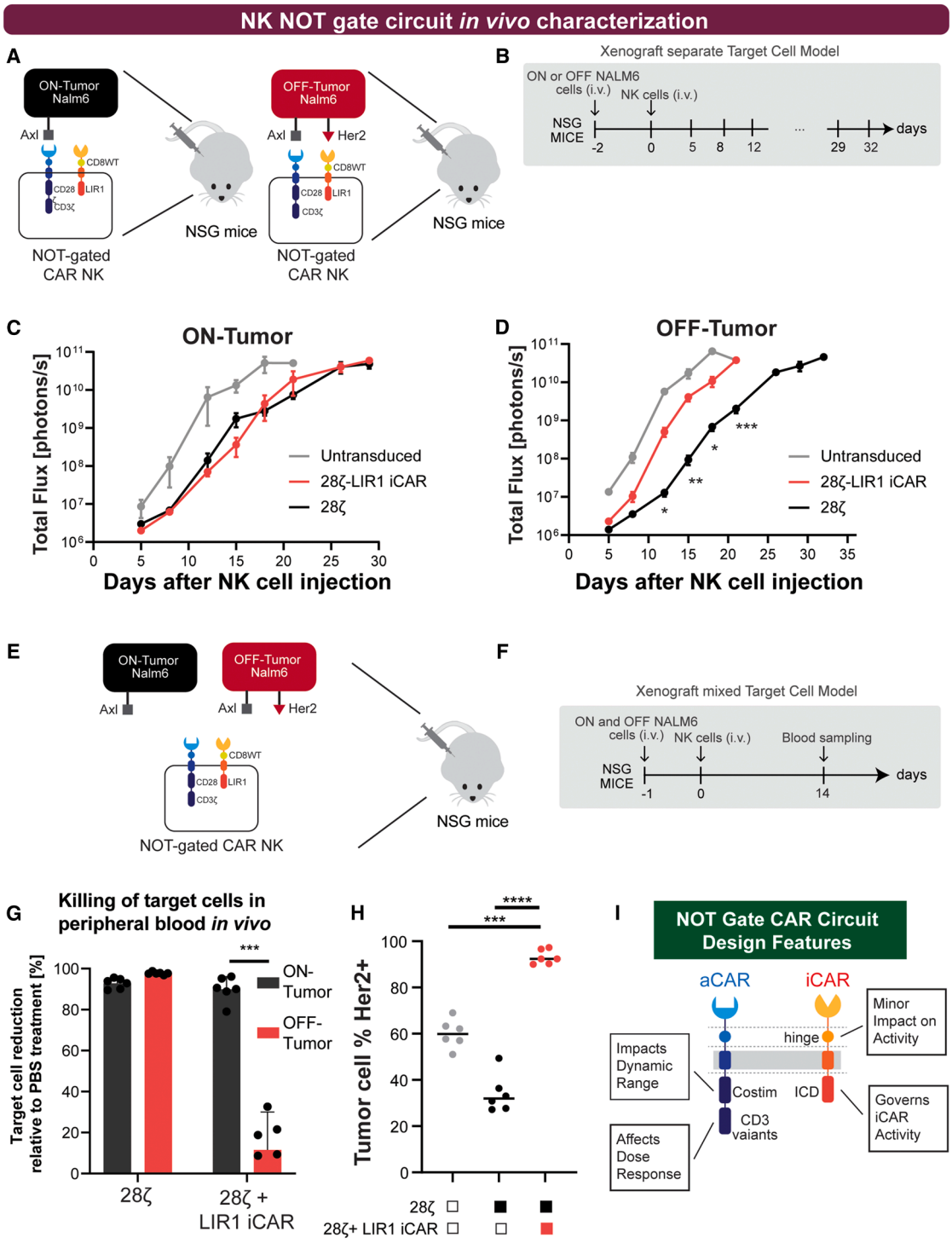

Figure 7. 28ζ-CD8WT hinge LIR1 iCAR NOT-gate circuit characterization in vivo with primary NK cells

(A) Schematics of single tumor xenograft mouse models with CAR-NK. ON-Tumor Nalm6 cells expressing the aCAR antigen Axl and OFF-Tumor Nalm6 cells expressing Axl and Her2 were injected into two distinct groups of mice.

(B) 2 days post-tumor injection, NK cells were treated in the mice. Tumor burden was measured with F-Luc activity from each tumor on the indicated dates.

(C) ON-Tumor burden measured after NK cell injection with the labeled group. 28ζ aCAR-only NK cells and 28ζ aCAR + CD8WT hinge LIR1 iCAR NOT-gated CAR NK cells did not show a discrepancy in killing against the ON-Tumor Nalm6 cells. $n = 2$ for all untransduced groups; $n = 3$ for 28ζ and 28ζ-LIR1 iCAR groups.

(D) OFF-Tumor burden measured after NK cell injection with the labeled group. 28ζ aCAR + CD8WT hinge LIR1 iCAR NOT-gate CAR NK cells limited the killing against the OFF-Tumor Nalm6 cells compared with the 28ζ transduced NK cells. $n = 2$ for all untransduced groups; $n = 4$ for 28ζ and 28ζ-LIR1 iCAR groups.

(legend continued on next page)

Please cite this article in press as: Lee et al., NOT-gated chimeric antigen receptor circuits in T and NK cells, Cell Systems (2026), https://doi.org/10.1016/j.cels.2026.101561

To further understand the design principle of the iCAR, we investigated the importance of hinge and transmembrane domains. We found that the hinge domain also has a significant but lesser role than the intracellular domain in determining iCAR activity, mirroring their role in aCAR designs. We also evaluated the paired aCAR and iCAR functionality for the complete NOT-gated CAR circuits. We learned that an unconventional version of the CD3ζ activation domain, CD3ζ(D23), leads to a sharper inhibition dose-response curve compared with other CD3ζ domains. Our 28ζ(D23) aCAR + LIR1 iCAR NOT-gated circuit in primary T cells demonstrated robust target discrimination *in vivo*. Furthermore, we also established the first NOT-gated CAR circuit in NK cells to show high performance in discriminated ON-Tumor vs. OFF-Tumor cells in a dual tumor model *in vivo*, in the context that the OFF-Tumor cells are not the NK cells as previously reported.[27] The direct portability of the NOT-gated CAR between T and NK cells is a pleasant surprise, which allowed us to leverage the robust genetic engineering tools available to T cells to rapidly screen for high-performing NOT-gated CAR and transfer a smaller subset to NK cells for further testings.

Natively, LIR1 is an inhibitory Ig superfamily receptor that binds to HLA-I. It is expressed on NK, T, B, and dendritic cells. One of the functions of LIR1 is to limit immune cell overactivation. LIR1 is a unique inhibitory receptor with four immunoreceptor tyrosine-based inhibitory motifs (ITIMs), the highest ITIM number in our iCAR collection. Whether all of the ITIMs on LIR1 are necessary for the iCAR performance has yet to be determined. However, duplicating the LIR1 domain on the iCAR led to lower expression and worse inhibition (data not shown). A more synthetic, non-canonical version of iCAR can be developed if the functionality of each ITIM is determined from the LIR1 domain.

It has been proposed that an aCAR with a costimulatory and a complete CD3ζ intracellular domain (with three ITAMs) may lead to overstimulation and exhaustion of T cells.[43] As such, mutations to the CD3ζ ITIM domains have been developed to limit the aCAR signaling. Sadelain and colleagues have shown that CARs containing only 1 ITAM (1XX or D23) have more potent anti-tumor activity in vivo than the CARs with three ITAMs. In this work, we showed that in addition to being more efficacious, the D23 mutant is also best inhibited by the LIR1 iCAR. We postulate that the first ITAM could be the preferred target of the LIR1 inhibition. The complete removal of the other two ITAM sequences on D23 may also eliminate competition to LIR1, thus enabling more efficient contact with LIR1. This work highlights the complex interplay between aCAR and iCAR and the importance of simultaneously interrogating both CARs to understand the property and potential of NOT-gated CAR circuits. The impacts of various design features of NOT-gated CAR circuits are summarized in Figure 7I.

From studying the mechanism of the LIR1 iCAR, we uncovered some interesting properties of the LIR1 iCAR. First, we learned that SHP-1 is the primary regulator, which is similar to BTLA but in contrast to PD-1.[58] We have also previously engineered an iCAR based on BTLA.[28] Whether iCAR that leverages SHP-1 as the primary regulator is more potent remains to be determined. We also confirmed through *in vitro* co-culture assay that LIR1 iCAR works in *cis* with aCAR, which requires the protective antigen to be expressed on the same cells as the target antigen to exert the inhibitory function. The requirement for *cis* function prevents healthy cells expressing the protective antigens from inhibiting the CAR T cell attacking the tumor cells (*trans*). This corroborates with our *in vivo* results showing that the presence of OFF-Target cells in the same place does not interfere with tumor killing. Finally, the expression of LIR1 iCAR reduces exhaustion phenotypes, demonstrating lower exhaustion marker expression and stronger cell killing. This provides another benefit of iCAR beyond improving tumor targeting specificity. Furthermore, this added benefit of exhaustion reduction has not been documented in the AND gate CAR circuit.

We performed our initial NOT-gated CAR screen in T cells because of the relative ease in genetic manipulation of T cells compared with NK cells. We have characterized their performance in T cells and identified key mechanistic insights using T cells. Nonetheless, it is remarkable that screening NOT-gate circuits in T cells also identifies functional NOT-gate circuits in NK cells. In a previous study, we reported that our NOT-gate circuits in NK cells can effectively discriminate between acute myeloid leukemia (AML) cells and healthy cells in a preclinical mouse model,[30] which has now been shown to have strong clinical efficacy in a phase 1 clinical trial for AML (5/7 complete remission). This highlights the portability and clinical potential of our NOT-gated CAR.

RESOURCE AVAILABILITY

Lead contact

Further information and requests for resources and reagents should be directed to and will be fulfilled by the lead contact, Wilson W. Wong (wilwong@bu.edu).

Materials availability

All plasmid constructs and cell lines generated in this study will be made available on request, but we may require a payment and/or a completed materials transfer agreement if there is potential for commercial application.

Data and code availability

All data reported in this paper will be shared by the lead contact upon request. This paper does not report original code. Any additional information required to reanalyze the data reported in this paper is available from the lead contact upon request.

(E) Schematics of dual tumor xenograft mouse models with CAR-NK. ON-Tumor Nalm6 cells expressing the aCAR antigen Axl and OFF-Tumor Nalm6 cells expressing Axl and Her2 were injected into the same group of mice.

(F) NK cells were injected 1 day post tumor injection, and blood samples were collected 14 days post-NK cell treatment.

(G) Blood samples were analyzed with fluorescence-activated cell sorting (FACS) to identify the remaining ON-Tumor and OFF-Tumor cells. The Her2+ cell numbers were normalized to the blood volume collected and the target cell number from the PBS-treated group. $n = 6$.

(H) Her2+ population among the tumor cells was measured from the collected blood sample 14 days post-treatment with the indicated NK cells. PBS-treated mice showed a 60% Her2+ population, the 28ζ NK-treated group showed a 32% population of Her2+ tumor cells, and the 28ζ-LIR1 iCAR NK-treated group showed 92% of the Her2+ population left. $n = 6$.

(I) Summary of how different CAR features affect NOT-gate CAR properties. For all data presented here, error bars represent ± standard deviation. Significance test, Student's *t* test; n.s., not significant; $^{*}p < 0.05$; $^{**}p < 0.01$; $^{***}p < 0.001$; $^{****}p < 0.0001$.

ACKNOWLEDGMENTS

W.W.W. acknowledges funding from Senti Biosciences and NIH awards (DP2CA186574, U01CA265713, and R01EB029483). We are grateful to Enfu Hui and his lab for kindly providing the Jurkat cell line with SHP1/SHP2 KO. We also thank Wong lab members for suggestions on the manuscript, Dr. Todd Blute from the BU Proteomics & Imaging Core Facility for flow cytometry assistance, and the BU IVIS imaging core facility for mice *in vivo* imaging (NIH grant 1S10RR024523-01).

AUTHOR CONTRIBUTIONS

S.L. designed and generated genetic constructs, performed experiments, analyzed the data, and generated figures. J. Chen helped to validate the iCAR functionality in T cells. M.Y.S. helped with *in vivo* mouse experiments with T cells and *in vitro* experiments with NK cells. J. Choi executed the Jurkat cell line experiment with SHP1/SHP2 KO, and J.H. contributed to the T cell exhaustion data. D.L., C.-T.L., N.A., M.T., and A.B. performed mouse experiments with NK cells and collected data, which was analyzed by D.L. and N.W.F. and supervised by N.W.F. and C.-T.L. N.W.F. designed the *in vivo* NK cell research strategy with input from M.G.A., R.G., and T.K.L. W.W.W. conceived and supervised the project and analyzed the data. All authors commented on and approved the paper.

DECLARATION OF INTERESTS

A patent application has been filed based on this work (S.L., W.W.W., R.G., M.G.A., and N.W.F.). W.W.W. is a scientific co-founder and shareholder of Senti Biosciences and 4Immune.

STAR★METHODS

Detailed methods are provided in the online version of this paper and include the following:

- KEY RESOURCES TABLE
- EXPERIMENTAL MODEL AND SUBJECT DETAILS
  - Source of Primary Human T Cells and NK cells
  - Animal Model Details
- METHOD DETAILS
  - CAR Constructs Design
  - Primary human T cell isolation and culture
  - Lentivirus generation and transduction
  - Cell line generation and culture
  - Antibodies
  - Antigen plate-bound assay
  - T cell cytotoxicity assay
  - Cytokine release assay
  - Xenograft mouse models
  - Primary NK cell extraction and culture
  - Cell line cultures
  - Retrovirus generation and transduction
  - CAR NK generation for xenograft mouse model
  - Xenograft mouse model for CAR-NK
- QUANTIFICATION AND STATISTICAL ANALYSIS

SUPPLEMENTAL INFORMATION

Supplemental information can be found online at https://doi.org/10.1016/j.cels.2026.101561.

Received: May 6, 2025
Revised: December 12, 2025
Accepted: February 18, 2026

REFERENCES

1. Liu, E., Marin, D., Banerjee, P., Macapinlac, H.A., Thompson, P., Basar, R., Nassif Kerbauy, L., Overman, B., Thall, P., Kaplan, M., et al. (2020). Use of CAR-Transduced Natural Killer Cells in CD19-Positive Lymphoid Tumors. N. Engl. J. Med. *382*, 545–553. https://doi.org/10.1056/NEJMoa1910607.
2. Pillai, A.B., George, T.I., Dutt, S., Teo, P., and Strober, S. (2007). Host NKT cells can prevent graft-versus-host disease and permit graft antitumor activity after bone marrow transplantation. J. Immunol. *178*, 6242–6251. https://doi.org/10.4049/jimmunol.178.10.6242.
3. Xu, Y., Xiang, Z., Alnaggar, M., Kouakanou, L., Li, J., He, J., Yang, J., Hu, Y., Chen, Y., Lin, L., et al. (2021). Allogeneic Vgamma9Vdelta2 T-cell immunotherapy exhibits promising clinical safety and prolongs the survival of patients with late-stage lung or liver cancer. Cell. Mol. Immunol. *18*, 427–439. https://doi.org/10.1038/s41423-020-0515-7.
4. Brudno, J.N., Somerville, R.P.T., Shi, V., Rose, J.J., Halverson, D.C., Fowler, D.H., Gea-Banacloche, J.C., Pavletic, S.Z., Hickstein, D.D., Lu, T.L., et al. (2016). Allogeneic T Cells That Express an Anti-CD19 Chimeric Antigen Receptor Induce Remissions of B-Cell Malignancies That Progress After Allogeneic Hematopoietic Stem-Cell Transplantation Without Causing Graft-Versus-Host Disease. J. Clin. Oncol. *34*, 1112–1121. https://doi.org/10.1200/JCO.2015.64.5929.
5. Eyquem, J., Mansilla-Soto, J., Giavridis, T., van der Stegen, S.J.C., Hamieh, M., Cunanan, K.M., Odak, A., Gönen, M., and Sadelain, M. (2017). Targeting a CAR to the TRAC locus with CRISPR/Cas9 enhances tumour rejection. Nature *543*, 113–117. https://doi.org/10.1038/nature21405.
6. Depil, S., Duchateau, P., Grupp, S.A., Mufti, G., and Poirot, L. (2020). 'Off-the-shelf' allogeneic CAR T cells: development and challenges. Nat. Rev. Drug Discov. *19*, 185–199. https://doi.org/10.1038/s41573-019-0051-2.
7. Makkouk, A., Yang, X.C., Barca, T., Lucas, A., Turkoz, M., Wong, J.T.S., Nishimoto, K.P., Brodey, M.M., Tabrizizad, M., Gundurao, S.R.Y., et al. (2021). Off-the-shelf Vdelta1 gamma delta T cells engineered with glypican-3 (GPC-3)-specific chimeric antigen receptor (CAR) and soluble IL-15 display robust antitumor efficacy against hepatocellular carcinoma. J. Immunother. Cancer *9*, e003441. https://doi.org/10.1136/jitc-2021-003441.
8. Yazdanifar, M., Barbarito, G., Bertaina, A., and Airoldi, I. (2020). gamma-delta T Cells: The Ideal Tool for Cancer Immunotherapy. Cells *9*, 1305. https://doi.org/10.3390/cells9051305.
9. Liu, S., Galat, V., Galat, Y., Lee, Y.K.A., Wainwright, D., and Wu, J. (2021). NK cell-based cancer immunotherapy: from basic biology to clinical development. J. Hematol. Oncol. *14*, 7. https://doi.org/10.1186/s13045-020-01014-w.
10. Curti, A., Ruggeri, L., D'Addio, A., Bontadini, A., Dan, E., Motta, M.R., Trabanelli, S., Giudice, V., Urbani, E., Martinelli, G., et al. (2011). Successful transfer of alloreactive haploidentical KIR ligand-mismatched natural killer cells after infusion in elderly high risk acute myeloid leukemia patients. Blood *118*, 3273–3279. https://doi.org/10.1182/blood-2011-01-329508.
11. Miller, J.S., Soignier, Y., Panoskaltsis-Mortari, A., McNearney, S.A., Yun, G.H., Fautsch, S.K., McKenna, D., Le, C., Defor, T.E., Burns, L.J., et al. (2005). Successful adoptive transfer and in vivo expansion of human haploidentical NK cells in patients with cancer. Blood *105*, 3051–3057. https://doi.org/10.1182/blood-2004-07-2974.
12. Ruggeri, L., Capanni, M., Urbani, E., Perruccio, K., Shlomchik, W.D., Tosti, A., Posati, S., Rogaia, D., Frassoni, F., Aversa, F., et al. (2002). Effectiveness of donor natural killer cell alloreactivity in mismatched hematopoietic transplants. Science *295*, 2097–2100. https://doi.org/10.1126/science.1068440.
13. Shah, N., Li, L., McCarty, J., Kaur, I., Yvon, E., Shaim, H., Muftuoglu, M., Liu, E., Orlowski, R.Z., Cooper, L., et al. (2017). Phase I study of cord blood-derived natural killer cells combined with autologous stem cell transplantation in multiple myeloma. Br. J. Haematol. *177*, 457–466. https://doi.org/10.1111/bjh.14570.

14. Kloss, C.C., Condomines, M., Cartellieri, M., Bachmann, M., and Sadelain, M. (2013). Combinatorial antigen recognition with balanced signaling promotes selective tumor eradication by engineered T cells. Nat. Biotechnol. *31*, 71–75. https://doi.org/10.1038/nbt.2459.

15. Lanitis, E., Poussin, M., Klattenhoff, A.W., Song, D., Sandaltzopoulos, R., June, C.H., and Powell, D.J., Jr. (2013). Chimeric antigen receptor T Cells with dissociated signaling domains exhibit focused antitumor activity with reduced potential for toxicity in vivo. Cancer Immunol. Res. *1*, 43–53. https://doi.org/10.1158/2326-6066.CIR-13-0008.

16. Wilkie, S., van Schalkwyk, M.C.I., Hobbs, S., Davies, D.M., van der Stegen, S.J.C., Pereira, A.C.P., Burbridge, S.E., Box, C., Eccles, S.A., and Maher, J. (2012). Dual targeting of ErbB2 and MUC1 in breast cancer using chimeric antigen receptors engineered to provide complementary signaling. J. Clin. Immunol. *32*, 1059–1070. https://doi.org/10.1007/s10875-012-9689-9.

17. Cho, J.H., Collins, J.J., and Wong, W.W. (2018). Universal Chimeric Antigen Receptors for Multiplexed and Logical Control of T Cell Responses. Cell *173*, 1426–1438.e11. https://doi.org/10.1016/j.cell.2018.03.038.

18. Lajoie, M.J., Boyken, S.E., Salter, A.I., Bruffey, J., Rajan, A., Langan, R.A., Olshefsky, A., Muhunthan, V., Bick, M.J., Gewe, M., et al. (2020). Designed protein logic to target cells with precise combinations of surface antigens. Science *369*, 1637–1643. https://doi.org/10.1126/science.aba6527.

19. Williams, J.Z., Allen, G.M., Shah, D., Sterin, I.S., Kim, K.H., Garcia, V.P., Shavey, G.E., Yu, W., Puig-Saus, C., Tsoi, J., et al. (2020). Precise T cell recognition programs designed by transcriptionally linking multiple receptors. Science *370*, 1099–1104. https://doi.org/10.1126/science.abc6270.

20. Roybal, K.T., Williams, J.Z., Morsut, L., Rupp, L.J., Kolinko, I., Choe, J.H., Walker, W.J., McNally, K.A., and Lim, W.A. (2016). Engineering T Cells with Customized Therapeutic Response Programs Using Synthetic Notch Receptors. Cell *167*, 419–432.e16. https://doi.org/10.1016/j.cell.2016.09.011.

21. Richards, R.M., Zhao, F., Freitas, K.A., Parker, K.R., Xu, P., Fan, A., Sotillo, E., Daugaard, M., Oo, H.Z., Liu, J., et al. (2021). NOT-Gated CD93 CAR T Cells Effectively Target AML with Minimized Endothelial Cross-Reactivity. Blood Cancer Discov. *2*, 648–665. https://doi.org/10.1158/2643-3230.BCD-20-0208.

22. Tao, L., Farooq, M.A., Gao, Y., Zhang, L., Niu, C., Ajmal, I., Zhou, Y., He, C., Zhao, G., Yao, J., et al. (2020). CD19-CAR-T Cells Bearing a KIR/PD-1-Based Inhibitory CAR Eradicate CD19(+)HLA-C1(-) Malignant B Cells While Sparing CD19(+)HLA-C1(+) Healthy B Cells. Cancers (Basel) *12*, 2612. https://doi.org/10.3390/cancers12092612.

23. Hamburger, A.E., DiAndreth, B., Cui, J., Daris, M.E., Munguia, M.L., Deshmukh, K., Mock, J.Y., Asuelime, G.E., Lim, E.D., Kreke, M.R., et al. (2020). Engineered T cells directed at tumors with defined allelic loss. Mol. Immunol. *128*, 298–310. https://doi.org/10.1016/j.molimm.2020.09.012.

24. Hwang, M.S., Mog, B.J., Douglass, J., Pearlman, A.H., Hsiue, E.H.C., Paul, S., DiNapoli, S.R., Konig, M.F., Pardoll, D.M., Gabelli, S.B., et al. (2021). Targeting loss of heterozygosity for cancer-specific immunotherapy. Proc. Natl. Acad. Sci. USA *118*, e2022410118. https://doi.org/10.1073/pnas.2022410118.

25. Fedorov, V.D., Themeli, M., and Sadelain, M. (2013). PD-1- and CTLA-4-based inhibitory chimeric antigen receptors (iCARs) divert off-target immunotherapy responses. Sci. Transl. Med. *5*, 215ra172. https://doi.org/10.1126/scitranslmed.3006597.

26. Sandberg, M.L., Wang, X., Martin, A.D., Nampe, D.P., Gabrelow, G.B., Li, C.Z., McElvain, M.E., Lee, W.H., Shafaattalab, S., Martire, S., et al. (2022). A carcinoembryonic antigen-specific cell therapy selectively targets tumor cells with HLA loss of heterozygosity in vitro and in vivo. Sci. Transl. Med. *14*, eabm0306. https://doi.org/10.1126/scitranslmed.abm0306.

27. Li, Y., Basar, R., Wang, G., Liu, E., Moyes, J.S., Li, L., Kerbauy, L.N., Uprety, N., Fathi, M., Rezvan, A., et al. (2022). KIR-based inhibitory CARs overcome CAR-NK cell trogocytosis-mediated fratricide and tumor escape. Nat. Med. *28*, 2133–2144. https://doi.org/10.1038/s41591-022-02003-x.

28. Cho, J.H., Okuma, A., Sofjan, K., Lee, S., Collins, J.J., and Wong, W.W. (2021). Engineering advanced logic and distributed computing in human CAR immune cells. Nat. Commun. *12*, 792. https://doi.org/10.1038/s41467-021-21078-7.

29. Bangayan, N.J., Wang, L., Burton Sojo, G., Noguchi, M., Cheng, D., Ta, L., Gunn, D., Mao, Z., Liu, S., Yin, Q., et al. (2023). Dual-inhibitory domain iCARs improve the efficiency of the AND-NOT gate CAR T strategy. Proc. Natl. Acad. Sci. USA *120*, e2312374120. https://doi.org/10.1073/pnas.2312374120.

30. Frankel, N.W., Deng, H., Yucel, G., Gainer, M., Leemans, N., Lam, A., Li, Y., Hung, M., Lee, D., Lee, C.T., et al. (2024). Precision off-the-shelf natural killer cell therapies for oncology with logic-gated gene circuits. Cell Rep. *43*, 114145. https://doi.org/10.1016/j.celrep.2024.114145.

31. Dannenfelser, R., Allen, G.M., VanderSluis, B., Koegel, A.K., Levinson, S., Stark, S.R., Yao, V., Tadych, A., Troyanskaya, O.G., and Lim, W.A. (2020). Discriminatory Power of Combinatorial Antigen Recognition in Cancer T Cell Therapies. Cell Syst. *11*, 215–228.e5. https://doi.org/10.1016/j.cels.2020.08.002.

32. Fujiwara, K., Tsunei, A., Kusabuka, H., Ogaki, E., Tachibana, M., and Okada, N. (2020). Hinge and Transmembrane Domains of Chimeric Antigen Receptor Regulate Receptor Expression and Signaling Threshold. Cells *9*, 1182. https://doi.org/10.3390/cells9051182.

33. Bister, A., Ibach, T., Haist, C., Smorra, D., Roellecke, K., Wagenmann, M., Scheckenbach, K., Gattermann, N., Wiek, C., and Hanenberg, H. (2021). A novel CD34-derived hinge for rapid and efficient detection and enrichment of CAR T cells. Mol. Ther. Oncolytics *23*, 534–546. https://doi.org/10.1016/j.omto.2021.11.003.

34. Zhang, A., Sun, Y., Du, J., Dong, Y., Pang, H., Ma, L., Si, S., Zhang, Z., He, M., Yue, Y., et al. (2021). Reducing Hinge Flexibility of CAR-T Cells Prolongs Survival In Vivo With Low Cytokines Release. Front. Immunol. *12*, 724211. https://doi.org/10.3389/fimmu.2021.724211.

35. Alabanza, L., Pegues, M., Geldres, C., Shi, V., Wiltzius, J.J.W., Sievers, S.A., Yang, S., and Kochenderfer, J.N. (2017). Function of Novel Anti-CD19 Chimeric Antigen Receptors with Human Variable Regions Is Affected by Hinge and Transmembrane Domains. Mol. Ther. *25*, 2452–2465. https://doi.org/10.1016/j.ymthe.2017.07.013.

36. Guedan, S., Calderon, H., Posey, A.D., Jr., and Maus, M.V. (2019). Engineering and Design of Chimeric Antigen Receptors. Mol. Ther. Methods Clin. Dev. *12*, 145–156. https://doi.org/10.1016/j.omtm.2018.12.009.

37. Muller, Y.D., Nguyen, D.P., Ferreira, L.M.R., Ho, P., Raffin, C., Valencia, R.V.B., Congrave-Wilson, Z., Roth, T.L., Eyquem, J., Van Gool, F., et al. (2021). The CD28-Transmembrane Domain Mediates Chimeric Antigen Receptor Heterodimerization With CD28. Front. Immunol. *12*, 639818. https://doi.org/10.3389/fimmu.2021.639818.

38. Hudecek, M., Sommermeyer, D., Kosasih, P.L., Silva-Benedict, A., Liu, L., Rader, C., Jensen, M.C., and Riddell, S.R. (2015). The nonsignaling extracellular spacer domain of chimeric antigen receptors is decisive for in vivo antitumor activity. Cancer Immunol. Res. *3*, 125–135. https://doi.org/10.1158/2326-6066.CIR-14-0127.

39. Hombach, A., Hombach, A.A., and Abken, H. (2010). Adoptive immunotherapy with genetically engineered T cells: modification of the IgG1 Fc 'spacer' domain in the extracellular moiety of chimeric antigen receptors avoids 'off-target' activation and unintended initiation of an innate immune response. Gene Ther. *17*, 1206–1213. https://doi.org/10.1038/gt.2010.91.

40. Almåsbak, H., Walseng, E., Kristian, A., Myhre, M.R., Suso, E.M., Munthe, L.A., Andersen, J.T., Wang, M.Y., Kvalheim, G., Gaudernack, G., et al. (2015). Inclusion of an IgG1-Fc spacer abrogates efficacy of CD19 CAR T cells in a xenograft mouse model. Gene Ther. *22*, 391–403. https://doi.org/10.1038/gt.2015.4.

41. Watanabe, N., Bajgain, P., Sukumaran, S., Ansari, S., Heslop, H.E., Rooney, C.M., Brenner, M.K., Leen, A.M., and Vera, J.F. (2016). Fine-tuning

the CAR spacer improves T-cell potency. Oncoimmunology *5*, e1253656. https://doi.org/10.1080/2162402X.2016.1253656.

42. Jonnalagadda, M., Mardiros, A., Urak, R., Wang, X., Hoffman, L.J., Bernanke, A., Chang, W.C., Bretzlaff, W., Starr, R., Priceman, S., et al. (2015). Chimeric antigen receptors with mutated IgG4 Fc spacer avoid fc receptor binding and improve T cell persistence and antitumor efficacy. Mol. Ther. *23*, 757–768. https://doi.org/10.1038/mt.2014.208.
43. Feucht, J., Sun, J., Eyquem, J., Ho, Y.J., Zhao, Z., Leibold, J., Dobrin, A., Cabriolu, A., Hamieh, M., and Sadelain, M. (2019). Calibration of CAR activation potential directs alternative T cell fates and therapeutic potency. Nat. Med. *25*, 82–88. https://doi.org/10.1038/s41591-018-0290-5.
44. Kouro, T., Himuro, H., and Sasada, T. (2022). Exhaustion of CAR T cells: potential causes and solutions. J. Transl. Med. *20*, 239. https://doi.org/10.1186/s12967-022-03442-3.
45. Meng, X., Jing, R., Qian, L., Zhou, C., and Sun, J. (2020). Engineering Cytoplasmic Signaling of CD28zeta CARs for Improved Therapeutic Functions. Front. Immunol. *11*, 1046. https://doi.org/10.3389/fimmu.2020.01046.
46. Wu, W., Zhou, Q., Masubuchi, T., Shi, X., Li, H., Xu, X., Huang, M., Meng, L., He, X., Zhu, H., et al. (2020). Multiple Signaling Roles of CD3epsilon and Its Application in CAR-T Cell Therapy. Cell *182*, 855–871.e23. https://doi.org/10.1016/j.cell.2020.07.018.
47. Su, Y., Walker, J.R., Park, Y., Smith, T.P., Liu, L.X., Hall, M.P., Labanieh, L., Hurst, R., Wang, D.C., Encell, L.P., et al. (2020). Novel NanoLuc substrates enable bright two-population bioluminescence imaging in animals. Nat. Methods *17*, 852–860. https://doi.org/10.1038/s41592-020-0889-6.
48. Taylor, A., Sharkey, J., Plagge, A., Wilm, B., and Murray, P. (2018). Multicolour In Vivo Bioluminescence Imaging Using a NanoLuc-Based BRET Reporter in Combination with Firefly Luciferase. Contrast Media Mol. Imaging *2018*, 2514796. https://doi.org/10.1155/2018/2514796.
49. Germain-Genevois, C., Garandeau, O., and Couillaud, F. (2016). Detection of Brain Tumors and Systemic Metastases Using NanoLuc and Fluc for Dual Reporter Imaging. Mol. Imaging Biol. *18*, 62–69. https://doi.org/10.1007/s11307-015-0864-2.
50. Lorenz, U. (2009). SHP-1 and SHP-2 in T cells: two phosphatases functioning at many levels. Immunol. Rev. *228*, 342–359. https://doi.org/10.1111/j.1600-065X.2008.00760.x.
51. Christofides, A., Katopodi, X.L., Cao, C., Karagkouni, D., Aliazis, K., Yenyuwadee, S., Aksoylar, H.I., Pal, R., Mahmoud, M.A.A., Strauss, L., et al. (2023). SHP-2 and PD-1-SHP-2 signaling regulate myeloid cell differentiation and antitumor responses. Nat. Immunol. *24*, 55–68. https://doi.org/10.1038/s41590-022-01385-x.
52. Maskalenko, N.A., Zhigarev, D., and Campbell, K.S. (2022). Harnessing natural killer cells for cancer immunotherapy: dispatching the first responders. Nat. Rev. Drug Discov. *21*, 559–577. https://doi.org/10.1038/s41573-022-00413-7.
53. Shimasaki, N., Jain, A., and Campana, D. (2020). NK cells for cancer immunotherapy. Nat. Rev. Drug Discov. *19*, 200–218. https://doi.org/10.1038/s41573-019-0052-1.
54. Matosevic, S. (2018). Viral and Nonviral Engineering of Natural Killer Cells as Emerging Adoptive Cancer Immunotherapies. J. Immunol. Res. *2018*, 4054815. https://doi.org/10.1155/2018/4054815.
55. Fei, F., Rong, L., Jiang, N., Wayne, A.S., and Xie, J. (2022). Targeting HLA-DR loss in hematologic malignancies with an inhibitory chimeric antigen receptor. Mol. Ther. *30*, 1215–1226. https://doi.org/10.1016/j.ymthe.2021.11.013.
56. Goodman, D.B., Azimi, C.S., Kearns, K., Talbot, A., Garakani, K., Garcia, J., Patel, N., Hwang, B., Lee, D., Park, E., et al. (2022). Pooled screening of CAR T cells identifies diverse immune signaling domains for next-generation immunotherapies. Sci. Transl. Med. *14*, eabm1463. https://doi.org/10.1126/scitranslmed.abm1463.
57. Gordon, K.S., Kyung, T., Perez, C.R., Holec, P.V., Ramos, A., Zhang, A.Q., Agarwal, Y., Liu, Y., Koch, C.E., Starchenko, A., et al. (2022). Screening for CD19-specific chimaeric antigen receptors with enhanced signalling via a barcoded library of intracellular domains. Nat. Biomed. Eng. *6*, 855–866. https://doi.org/10.1038/s41551-022-00896-0.
58. Xu, X., Hou, B., Fulzele, A., Masubuchi, T., Zhao, Y., Wu, Z., Hu, Y., Jiang, Y., Ma, Y., Wang, H., et al. (2020). PD-1 and BTLA regulate T cell signaling differentially and only partially through SHP1 and SHP2. J. Cell Biol. *219*, e201905085. https://doi.org/10.1083/jcb.201905085.
59. Cho, J.H., Okuma, A., Al-Rubaye, D., Intisar, E., Junghans, R.P., and Wong, W.W. (2018). Engineering Axl specific CAR and SynNotch receptor for cancer therapy. Sci. Rep. *8*, 3846. https://doi.org/10.1038/s41598-018-22252-6.

Please cite this article in press as: Lee et al., NOT-gated chimeric antigen receptor circuits in T and NK cells, Cell Systems (2026), https://doi.org/10.1016/j.cels.2026.101561

STAR★METHODS

KEY RESOURCES TABLE

REAGENT or RESOURCE	SOURCE	IDENTIFIER
Antibodies		
APC-Cy7-anti-human CD69	BD Pharmingen	RRID: AB_396862; 557756
Axl APC-conjugated Antibody	R&D Systems	RRID: AB_2934005; FAB154A
FITC anti-human CD340 (erbB2/HER-2) antibody	BioLegend	RRID: AB_756120; 324404
Myc-Tag (9B11) Mouse mAb (Alexa Fluor® 647 Conjugate)	Cell Signaling Technology	RRID: AB_823474; 2233
V5 Tag Monoclonal Antibody, FITC	ThermoFisher	RRID: AB_2556567; R963-25
OKT-3	ThermoFisher	RRID: AB_467057; 14-0037-82
anti-CD3 antibody	BioLegend	RRID: AB_493693; 300322 / 300312
anti-CD56 antibody	BioLegend	RRID: AB_2564084; 362511 / 362545
mouse anti-human CD107a-APC antibody	BD Biosciences	RRID: AB_1645722; 641581
anti-TNFα-PE	BioLegend	RRID: AB_315261; 502909
anti-human IFNγ-FITC antibody	BioLegend	RRID: AB_315231; 502506
Cell Culture Reagents		
X-VIVO 15	Lonza	04-418Q
Human AB serum	Valley Medical	HP1022
N-acetyl L-Cysteine	Sigma-Aldrich	A9165
2-Mercaptoethanol	Thermo Fisher Sci-entific	21985023
IL-2	NCI BRB Preclinical Repository	N/A
Freestyle 293 Expression Medium	Fisher Scientific	12-338-026
DMEM	Corning	10-013
FBS	Thermo Fisher	10437028
penicillin/streptomycin	Corning	30001CI
L-glutamine	Corning	25005CI
sodium pyruvate	Lonza	13115E
Puromycin	Thermo Scientific	A1113803
Zeocin	Thermo Scientific	R25005
Hygromycin B	Thermo Fisher	10687010
NK MACS media	Miltenyi Biotech	130-114-429
CTS NK-Xpander media	ThermoFisher	A5019001
OptiPRO SFM	ThermoFisher	12309-019
Chemicals, peptides, and recombinant proteins		
ImmunoCult™ Human CD3/CD28 T Cell Activator	STEMCELL	10971
RetroNectin® Recombinant Human Fibronectin Fragment	Takara Bio	T100B
Puromycin	Thermo Scientific	A1113803
human Her2/ErbB2 protein	Sino biological	10004-H08H
Axl kinase protein (ECD, His Tag)	Sino biological	10279-H08H
SYTOX™ Red Dead Cell Stain	Invitrogen	S34859
IVISbrite D-Luciferin Potassium Salt Bioluminescent Substrate	PerkinElmer	122799
mitomycin C	Cayman Chemical Company	11435
GolgiPlug	BD Biosciences	555029
GolgiStop	BD Biosciences	554724
D-luciferin	Gold Biotechnology Inc	LUCK-5G
RBC lysis buffer	Biolegend	420302
PEG8000	Thermo Fisher Sci-entific	BP233-1
Sodium Chloride	Thermo Fisher Sci-entific	AAJ2161836

(*Continued on next page*)

Please cite this article in press as: Lee et al., NOT-gated chimeric antigen receptor circuits in T and NK cells, Cell Systems (2026), https://doi.org/10.1016/j.cels.2026.101561

Continued

REAGENT or RESOURCE	SOURCE	IDENTIFIER
RBC lysis buffer	Biolegend	420302
Critical commercial assays		
RosetteSep™ Human T Cell Enrichment	STEMCELL Tech-nologies	15021
CellTrace™ Violet Cell Proliferation Kit, for flow cy-tometry	Thermo Fisher Sci-entific	C34557
PiggyBac Transposon system	System Biosciences	N/A
Human IL-2 ELISA Set	BD Biosciences	555190
Human IFN-γ ELISA Set	BD Biosciences	555142
FuGENE HD transfection reagent	Promega	E2312
Human NK Cell Isolation Kit	Miltenyi Biotech	130-092-657
Fixation/Permeabilization Solution Kit	BD Biosciences	554715
Experimental models: Cell lines		
HEK293FT	N/A	N/A
GP2-293	Takara Bio	631530
HT-1080	N/A	N/A
Nalm6	ATCC	CRL-3273
RS4(11)	ATCC	CRL1873
NK cells	Senti Biosciences	N/A
Axl+ Nalm6	This paper	N/A
Axl+ Her2+ Nalm6	This paper	N/A
Experimental models: Organisms/strains		
Female NSG mice	Jackson Laboratories	005557
hIL-15 NOG	Taconic	13683-F
Recombinant DNA		
pHR-SFFV vector	Addgene	79121
Software and algorithms		
SpectraMax M5	Molecular Devices	N/A
FlowJo V10	FlowJo	N/A
GraphPad Prism 9	GraphPad	N/A

EXPERIMENTAL MODEL AND SUBJECT DETAILS

Source of Primary Human T Cells and NK cells

Blood collars were obtained from the Blood Donor Center at Boston Children's Hospital (Boston, MA) from anonymous healthy donors, with no identifiable private information collected, and thus not deemed human subjects research under 45 CFR 46.102(e).

Animal Model Details

T cell in vivo experiments were conducted at the Boston University Medical School Animal Science Center (BUASC) following the protocol approved by the Institutional Animal Care and Use Committee (PROTO201800600). Female NOD.Cg-Prkdc^{scid} Il2rg^{tm1Wjl}/SzJ (NSG) mice were purchased from 6-10 week of age from Jackson Laboratories (#005557). The mice were not exposed to any previous treatment before the experiment and housed in sterile cages at BUASC with 12 hour light/dark cycle. The mice were monitored daily by BUASC husbandry staff before and after the experiment until euthanization. When mice showed signs of illness such as loss of weight more than 10% in a week, or 15% of the maximum weight, hunched posture, impaired mobility, rough coat, they were euthanized.

METHOD DETAILS

CAR Constructs Design

iCARs were designed by combining the scFv, hinge, transmembrane domain, and intracellular domain, further connected with T2A-puroR gene segments. scFvs were adopted from previous papers,[17,28,59] hinge domains were implemented from previous CAR papers (ref) or from native domains obtained from UniProt. Transmembrane and intracellular domains were introduced from the candidate proteins, which sequences are also obtained from UniProt.

Please cite this article in press as: Lee et al., NOT-gated chimeric antigen receptor circuits in T and NK cells, Cell Systems (2026), https://doi.org/10.1016/j.cels.2026.101561

aCAR designs were mainly adopted from the previous papers.[17,43,46] Domains were analyzed, mutated/deleted if applicable, and codon-optimized before construction.

Primary human T cell isolation and culture

Primary peripheral blood mononuclear cells (PBMCs) were obtained from healthy donors at the Blood Donor Center at Boston Children's Hospital (Boston, MA) as approved by the Boston University Institutional Review Board (IRB). T cells were isolated using RosetteSep™ Human T Cell Enrichment Cocktail (STEMCELL, #15021) according to the manufacturer's protocol. Isolated primary T cells were either maintained fresh or stored as cell stocks in liquid nitrogen. T cells were maintained in X-Vivo 15 media (Lonza, # 04-418Q) supplemented with 5% human AB serum (Valley Biomedical, #HP1022), 10mM N-acetyl L-Cysteine (Sigma, #A9165), 55μM 2-Mercaptoethanol (Thermo Fisher, #21985023), and 50-300 U/ml IL-2 (NCI BRB Preclinical Repository). Every 2 days, the cells were counted and maintained at 500k cells/ml to 1,000,000 cells/ml concentrations.

Lentivirus generation and transduction

pHR lentiviral vectors with pDelta, pAdv packaging plasmid, and Vsvg envelope plasmid were used to generate lentivirus. The packaging and transfer plasmids were transfected with polyethylenimine (PEI) into the HEK293FT cell line. 24 hours after transfection, culture media was completely changed with Freestyle 293 Expression Medium (Fisher Scientific, # 12-338-026) then collected twice at 48 hours and 72 hours after the transfection. The collected virus was mixed with 40% PEG-8000 solution at a 3:1 ratio of virus:concentrator overnight at 4C, spun down for concentration of the virus at 1600g for 60 minutes to the desired amount. The concentrated virus was stored in -80 °C until usage.

Isolated primary T cells were thawed two days before transduction and activated with ImmunoCult™ Human CD3/CD28 T Cell Activator (STEMCELL, #10971) 24 hours before transduction. For transduction, retronectin (Takara Bio #T100B) was coated at a 32ng/ml concentration in either 24-well non-TC treated plates or 6-well non-TC treated plates overnight at 4 °C. Retronectin was removed, wells were blocked with 1% Bovine Serum Albumin concentration for 30 minutes at room temperature, and the virus was added to each well then spun at 1200g for 90 minutes. After spinning down the virus, the remaining liquid was suctioned out, and then T cells were added at 250k cells/ml concentration with 300 IU/ml of IL-2 supplement. The transduced T cells were washed with fresh media with 100IU/ml IL-2 72 hours after the transduction. To select for iCAR+ population after co-transduction, 2 μg/ml of Puromycin (Thermo Scientific #A1113803) was added 72 hours post-transduction and maintained until assays were performed on the T cells.

Cell line generation and culture

HEK293FT, HT-1080, and GP2-293 (Takara Bio # 631530) cell lines used for retrovirus generation were cultured and maintained in Dulbecco's modified Eagle's medium (DMEM) supplemented with 10% fetal bovine serum (FBS; Thermo Fisher, 10437028), penicillin/streptomycin (Corning, 30001CI), L-glutamine (Corning, 25005CI) and 1mM sodium pyruvate (Lonza, 13115E). Nalm6 cells and RS4(11) cells were purchased from ATCC and maintained in RPMI 1640 supplemented with 10% FBS, 2 mM L-glutamine, 10 mM HEPES, 1 mM sodium pyruvate, 4500 mg/L glucose, and 1500 mg/L sodium bicarbonate. For labeling of Nalm6 cells, the PiggyBac Transposon system (System Biosciences) was used to encode BFP and luciferase with a zeocin resistance gene tagged. Both Axl+ Nalm6 and Axl+ Her2+ Nalm6 were generated using lentivirus encoding truncated versions of Axl and Her2, missing the intracellular part of each antigen. Generated Nalm6 cell lines were used for up to 2 months and discarded. For antibiotic selection, Puromycin (Thermo Scientific, #A1113803), Zeocin (Thermo Scientific, # R25005), or Hygromycin B (Thermo Fisher #10687010) was added to the medium to select for transduced cells.

Antibodies

CD69 readout was measured with APC-Cy7-conjugated mouse anti-human CD69 antibody (BD Pharmingen, #557756) at a dilution ratio of 1:200. To check the antigen expression level, human Axl APC-conjugated Antibody (R&D Systems, #FAB154A) was used at a dilution ratio of 1:200 and FITC anti-human CD340 (erbB2/HER-2) antibody (BioLegend, #324404) was used at 1:200. To check the aCAR and iCAR expression level, Myc-Tag (9B11) Mouse mAb (Alexa Fluor® 647 Conjugate) (Cell Signaling Technology, #2233S) was used at 1:200, and V5 Tag Monoclonal Antibody, FITC (ThermoFisher, #R963-25) was used at a 1:500 dilution ratio.

Cells were spun down and washed with PBS for the surface staining, then stained with antibodies at desired dilution with FACS buffer (1x phosphate buffered saline (PBS), 0.1% NaN3, 1% BSA 2mM EDTA) in the dark at room temperature for 30 minutes. Cells were then washed with PBS again and resuspended with FACS buffer for analysis on the Attune NxT flow cytometer.

Antigen plate-bound assay

Lyophilized target proteins, human Her2/ErbB2 protein (Sino biological, #10004-H08H) and human Axl kinase protein (ECD, His Tag) (Sino biological, #10279-H08H) were resuspended in distilled water at the concentration instructed by the manufacturer and diluted at the desired concentration in PBS. For antigen protein adsorption, either non-TC treated 96-well flat bottom plates or 96-well MaxiSorp plates (ThermoFisher, #442404) were used. The diluted antigen was added to the wells in 200 μl of total volume, then incubated at 4 °C overnight.

Please cite this article in press as: Lee et al., NOT-gated chimeric antigen receptor circuits in T and NK cells, Cell Systems (2026), https://doi.org/10.1016/j.cels.2026.101561

T cell cytotoxicity assay

For the killing assay, both T cells and Nalm6 cells were washed with RPMI with 5% FBS and incubated in 96-well V-bottom plates at the desired E:T ratio overnight in a 37°C incubator. After incubation, the supernatant was collected to perform an ELISA assay, and cells were resuspended with FACS buffer containing SYTOX™ Red Dead Cell Stain (Invitrogen, #S34859). The samples were analyzed on the Attune NxT flow cytometer to count the remaining live Nalm6 cell number by gating SYTOX Red negative, BFP positive population. Lysis% of the target was calculated as the percentage of cells killed normalized to the cell number from the wells containing Nalm6 alone.

Cytokine release assay

Supernatant collected from the killing assays was preserved at -80 °C until the enzyme-linked immunosorbent assay (ELISA) was performed. To measure IFNγ, IL-2, and TNF-α secretion, BD OptEIA human IFNγ, IL-2 ELISA kits (BD Biosciences, 555142, 555190, 555212) were used following manufacturer's instructions with BD OptEIA Reagent Set B (BD Biosciences, 550534) and measured with SpectraMax M5 (Molecular Devices).

Xenograft mouse models

Female NSG mice, 8-10 weeks of age, were purchased from Jackson Laboratories (#005557) and maintained in the BUMC Animal Science Center (ASC). All animal experiment protocols were approved by the Institutional Animal Care and Use Committee at BUMC. 500k Nalm6 cells expressing firefly luciferase (F-Luc) and target antigen were injected intravenously. 4 days after, CAR-transduced T cells were injected intravenously. Tumor burden was measured with IVIS Spectrum (Xenogen) within 10 minutes of intraperitoneally injecting IVISbrite D-Luciferin Potassium Salt Bioluminescent Substrate (PerkinElmer, #122799). The amount of tumor burden was quantified as total flux (photons per sec).

Primary NK cell extraction and culture

NK cells and autologous apheresis cells were obtained from Senti Biosciences. They were isolated from blood using the Human NK Cell Isolation Kit (130-092-657, Miltenyi Biotech) via autoMACS system (Miltenyi Biotech) and shipped to us overnight. The feeder cells were prepared as described before by irradiating the apheresis cells from the same donor as the NK cells. The apheresis cells were irradiated by either XRad 320 or MultiRad 350 (Precision X-ray) with 20 Gy under the indicated filter. If mitomycin C (Cayman Chemical Company #11435) was used to arrest the cell cycle of the apheresis cells, the apheresis cells were treated with the indicated concentration of mitomycin C, cultured for a day, washed twice with fresh media, then mixed with NK cells. NK cells were mixed with the feeder cells at a 1:5 ratio of NK cell:feeder cells in NK MACS media (Miltenyi Biotech #130-114-429) or CTS NK-Xpander media (ThermoFisher #A5019001) supplemented with 5% human AB serum (Valley Biomedical #HP1022) and 500 IU/ml of human IL-2 (NCI BRB Preclinical Repository) with 10ng/ml of OKT-3 (ThermoFisher #14-0037-82). The percentage of NK cells and T cells was checked with anti-CD3 antibody (BioLegend #300322 or # 300312) and anti-CD56 antibody (BioLegend #362511 or # 362545) on the indicated dates. Primary NK cells were maintained between 400k cells/ml to 3 million cells/ml from day 5 of the co-culture.

Cell line cultures

HEK293FT, HT-1080, and GP2-293 (Takara Bio # 631530) cell lines used for retrovirus generation were cultured and maintained in Dulbecco's modified Eagle's medium (DMEM) supplemented with 10% fetal bovine serum (FBS; Thermo Fisher, 10437028), penicillin/streptomycin (Corning, 30001CI), L-glutamine (Corning, 25005CI) and 1mM sodium pyruvate (Lonza, 13115E). Nalm6 cells and RS4(11) cells were purchased from ATCC and maintained in RPMI 1640 supplemented with 10% FBS, 2 mM L-glutamine, 10 mM HEPES, 1 mM sodium pyruvate, 4500 mg/L glucose, and 1500 mg/L sodium bicarbonate.

Retrovirus generation and transduction

Retrovirus was generated using the GP2-293 cell line. pMX Transfer vectors and BaEVTR envelope vectors were mixed at a 3:1 weight ratio, transfected with PEI as described in lentiviral vector transfection or with FuGENE HD transfection reagent (Promega # E2312). 24 hours after transfection, the culture media was completely changed with OptiPRO SFM (ThermoFisher # 12309-019), then collected at 48 hours and 72 hours after transfection. Spinfection was used to transduce NK cells with retrovirus, as described previously. All aCARs and iCARs were transduced into NK cells using retrovirus.

CAR NK generation for xenograft mouse model

NK cells were transduced with lentivirus of pL17d anti-Axl-28z aCAR and/or pL17d anti-Axl-28z aCAR P2A anti-Her2-LIR1 iCAR. 500k cells were transduced with 250k pg/mL of virus and spun at 1200g for 90 mins in a non-TC treated 12-well dish coated with retronectin (Takara Bio T100B) as per manufacturer protocols. NK cells were transduced in NK Macs media (Miltenyi 130-114-429), supplemented with 10% human Ab serum (Valley Biomedical HP1022HI), 1% NK Macs supplement, 500 U IL-2/mL, and 10 ng IL-15/mL. Volume per well was 1 mL during spinoculation, and 1 mL of complete NK MACS media was added post spin. 7 days post transduction, cells were transferred to a 6M G-Rex (Wilson Wolf 80660M) and seeded at a density of 5 million cells per well in 100 mL of complete NK Macs media. NK cells were grown for 14 days, and 500U IL-2/mL and 10ng IL-15 were added 2 times a week.

Please cite this article in press as: Lee et al., NOT-gated chimeric antigen receptor circuits in T and NK cells, Cell Systems (2026), https://doi.org/10.1016/j.cels.2026.101561

Xenograft mouse model for CAR-NK

NK cells were harvested after 14 days, washed twice, and resuspended in PBS. NK cells were resuspended at 10 million per 150 μL and injected IV on either day 1 or day 2 after NALM6 engraftment. NK cells were administered to NSG-TG(Hu-Il15) mice (Jackson Labs strain #030890).

NALM6 cells were washed twice and resuspended in PBS. NALM6 cells were resuspended at 500k cells per 50uL of volume and injected IV on day 0. Bioluminescence imaging was performed using a Lago Imager (Spectral Instruments). The mice were injected with 200 μl of D-luciferin (150mg/kg) (Gold Biotechnology Inc, LUCK-5G) and imaged 10 minutes later. Peripheral blood was collected by submental bleeding 1 time a week in an EDTA tube, of which 150 μL per mouse was processed for flow cytometry. Blood was lysed with RBC lysis buffer (Biolegend 420302) following manufacturer protocols and stained for 1 hour with either of the following antibody panels.

QUANTIFICATION AND STATISTICAL ANALYSIS

Data between the two groups were compared using an unpaired two-tailed t-test. All curve fitting was performed with Prism 9 (Graphpad), and p values are reported (not significant = $p > 0.05$, * = $p < 0.05$, ** = $p < 0.01$, *** =$p < 0.001$). All error bars are represented as either SEM or SD.